

Inhomogeneous systems with unusual critical behaviour

F Iglói[†], I Peschel[‡] and L Turban[§]

[†] *Research Institute for Solid State Physics, P. O. Box 49
H-1525 Budapest 114, Hungary*

[‡] *Fachbereich Physik, Freie Universität Berlin, Arnimallee 14
D-14195 Berlin, Germany*

[§] *Laboratoire de Physique du Solide, URA CNRS 155, Université de Nancy I, BP239
F-54506 Vandœuvre lès Nancy cedex, France*

Abstract: The phase transitions and critical properties of two types of inhomogeneous systems are reviewed. In one case, the local critical behaviour results from the particular shape of the system. Here scale-invariant forms like wedges or cones are considered as well as general parabolic shapes. In the other case the system contains defects, either narrow ones in the form of lines or stars, or extended ones where the couplings deviate from their bulk values according to power laws. In each case the perturbation may be irrelevant, marginal or relevant. In the marginal case one finds local exponents which depend on a parameter. In the relevant case unusual stretched exponential behaviour and/or local first order transitions appear. The discussion combines mean field theory, scaling considerations, conformal transformations and perturbation theory. A number of examples are Ising models for which exact results can be obtained. Some walks and polymer problems are considered, too.

22 August 2018

Accepted for publication in Advances in Physics.

[†] *igloi@power.szfki.kfki.hu*

[‡] *peschel@aster.physik.fu-berlin.de*

[§] *turban@lps.u-nancy.fr*

Contents

	Page
1. Introduction	3
2. Planar surfaces	5
2.1. Mean field theory	5
2.2. Correlation functions and critical profiles	9
2.3. Surface exponents	12
3. Wedges, corners and cones	14
3.1. Mean field theory	15
3.2. Ising models	17
3.3. Other systems	19
3.4. Conformal results	20
4. Parabolic shapes	23
4.1. Mean field theory	23
4.2. Conformal and scaling results	25
4.3. Ising model	27
4.4. Other systems	28
5. Extended defects at surfaces	31
5.1. Ising model, general results	31
5.2. Ising model boundary magnetization	33
5.3. Conformal invariance for the marginal case	35
5.4. Related problems	36
5.5. Scaling considerations for relevant inhomogeneities	38
6. Narrow line defects in the bulk	40
6.1. Mean field theory and scaling	40
6.2. Ising model with a defect line	41
6.3. Conformal invariance, star-like defects	45
7. Extended defects in the bulk	47
7.1. Ising model, conformal results	48
8. Radially extended defects	50
8.1. Scaling considerations	50
8.2. Ising model	50
8.3. Conformal considerations	52
9. Conclusion	53
Acknowledgments	54
Appendix A. Scaling and conformal invariance	55

A.1. Scaling and critical exponents	55
A.2. Conformal invariance	57
Appendix B. Transfer matrices	60
B.1. Row transfer matrix	61
B.2. Corner transfer matrix	63
B.3. Rescaling	65
Appendix C. Perturbation theory for extended defects	66
C.1. General	66
C.2. Relevance-irrelevance criterion	67
C.3. Marginal behaviour	68
References	71

1. Introduction

In all fields of physics homogeneous systems have the simplest properties and thus play a particular rôle. This also holds with respect to phase transitions and critical phenomena. The general behaviour, the universal features near second-order transitions and the universality classes in this case are well-known [1]. On the other hand, all real systems are inhomogeneous in one way or another. This may affect their properties in different ways. Enhanced couplings in a finite region of a ferromagnetic system will result in a locally stronger magnetic order. For the case of competing interactions the effects of an inhomogeneity may be more complicated in detail but will still be of a local and quantitative nature. If, however, the perturbation has sufficient extent, the character of the phase transition and the critical behaviour may change.

One example for this situation is well-known: a system with a free surface. To obtain it from a homogeneous system one has to cut an infinite number of bonds. The case of planar surfaces was first treated for the two-dimensional Ising model [2, 3] and subsequently studied in great detail [4, 5]. It was found that, connected with the surface, there is a set of critical exponents with values different from those in the bulk. The modified critical behaviour is seen in a boundary layer which has a width of the order of the correlation length.

The planar surface, however, is only the simplest example showing such an effect. A number of other inhomogeneous systems display similar features. It is then of interest to collect and present these cases, to see relations between them and to discuss the basic aspects and mechanisms. This is the aim of the following review.

The systems to be discussed are mainly classical spin systems with short-range ferromagnetic interactions and, occasionally, walks and polymers. The inhomogeneities have a regular, non-random nature and the examples fall into two groups. One consists of systems in various geometrical forms with free boundaries described by algebraic curves, the other contains models with defect lines or extended inhomogeneities with algebraically varying strength. In both cases unusual and nonuniversal critical behaviour is found if the perturbation is sufficiently effective. Then the local exponents depend continuously on a parameter or the behaviour changes altogether from power laws to stretched exponentials. In the second group of systems also local ordering at or above the bulk transition temperature may occur. The necessary condition for these effects always involves scaling dimensions of the undisturbed system.

There are homogeneous systems which also show such features. An example is the eight-vertex model [6]. In this case, however, all exponents vary in a similar way and one can obtain universal values by measuring the temperature via the correlation length.

The inhomogeneous systems considered here have a richer structure since local and bulk quantities appear simultaneously. In those cases where the effects are related to the geometry they also are of a rather general nature since non-universal behaviour occurs for any simple isotropic system and in all dimensions.

The mentioned phenomena can often already be seen in a mean field treatment which is therefore given in various places. More generally, renormalization and scaling considerations allow to classify the perturbations and the way they act. There also is a rather general method to calculate the change of critical exponents via perturbation theory. A majority of the examples are two-dimensional systems and for them two other methods are available. Conformal invariance makes detailed predictions at the critical point and has been used in various cases although its validity in inhomogeneous systems is not necessarily guaranteed. Exact calculations for various Ising systems, however, have always confirmed conformal results. Moreover they allow to obtain a complete picture by giving results for all temperatures. The main tool here are transfer matrices and the two-dimensional problems are thereby related to certain quantum spin chains. All these topics are treated in the various sections and in three appendices. The latter contain some background material and some more technical aspects.

Certain types of inhomogeneity will not be considered here although they may lead to interesting effects. Random systems, by their very nature, demand special methods and are still under investigation with respect to their critical properties. For reviews we refer to [7, 8]. In the case of wetting phenomena one is concerned with the properties of interfaces which are created by appropriate boundary conditions and which may be influenced by inhomogeneities. This is also a field in itself and has already been reviewed [9–11]. Finally, layered systems with a periodic structure [12–14] will also be omitted.

Some of the effects to be discussed should be observable in experiments but the article deals with the theoretical aspects. Nevertheless, it is not aimed at the specialist. The notation has thus been chosen as simple and coherent as possible and therefore differs from the usual one in some places.

2. Planar surfaces

At a free surface missing bonds reduce the order and, as mentioned before, the critical behaviour is modified locally. The loss of full translational invariance leads to a decay of correlations which is different parallel and perpendicular to the surface. In dimensions higher than two, enhanced surface couplings may induce surface order above the bulk critical temperature. The local critical behaviour can also be influenced by the surface geometry or through the introduction of long-range surface induced perturbations. These last two points will be considered in the next sections.

The easiest approach to the problem at hand makes use of mean field theory which often brings a good qualitative description of the phenomena and becomes exact above the upper critical dimension where the fluctuation effects are negligible. Since a detailed account of planar surface critical behaviour within this frame can be found elsewhere [15, 4] we limit ourselves to a brief study of the bulk transition and the ordinary surface transition for illustrative purpose. This will serve as an introduction to the mean field treatment of the other, less usual, inhomogeneous systems which are considered in the next sections.

There also exists a number of recent reviews dealing with surface critical behaviour beyond mean field theory [4, 5, 16, 17]. As a consequence, only selected results concerning the structure of correlations, critical profiles and surface exponents are discussed in this section.

2.1. Mean field theory

In Landau mean field theory the system is treated in a continuum description. The total free energy F of a system with a volume (V) limited by a surface (S) is written as the sum of bulk and surface contributions which are functionals of the order parameter $m(\mathbf{r})$ which is nonvanishing in the ordered phase

$$F[m] = \int_{(V)} f_b[m] \, dV + \int_{(S)} f_s[m] \, dS. \quad (2.1)$$

Let us consider for simplicity an Ising system with a scalar order parameter m and a free energy which in zero external field is even in m , i.e. symmetric under order parameter reversal. Near a second order transition, the order parameter is small and the bulk free energy density $f_b[m]$ is written as an expansion in the order parameter and its gradient, limited to the following terms

$$f_b[m] = f_b[0] + \frac{1}{2} C(\nabla m)^2 + \frac{1}{2} A m^2 + \frac{1}{4} B m^4 - h m. \quad (2.2)$$

The second one, with $C > 0$, gives the extra energy associated with a spatial variation of the order parameter, $A \sim T - T_c$ measures the deviation from the critical temperature T_c , B is a positive constant to ensure stability below T_c and h is the bulk external field.

In the same way the surface free energy density is written phenomenologically as

$$f_s[m] = f_s[0] + \frac{1}{2} C \frac{m^2}{\Lambda} - h_s m \quad (2.3)$$

where m is the value of the order parameter on (S) . The quantity Λ , with the dimension of a length, is called the extrapolation length and can be deduced from the microscopic surface and bulk interactions through a mean field treatment of the microscopic Hamiltonian of the system [4].

The equilibrium value of the order parameter $m(\mathbf{r})$ minimizes the free energy in (2.1). It may be obtained through a variational calculation by looking for the first order change of the free energy, $\delta F[m]$, associated with a deviation $\delta m(\mathbf{r})$ of the order parameter from its equilibrium value. Using (2.1–3), one obtains

$$\begin{aligned} \delta F[m] = & \int_{(V)} [C \nabla m \cdot \nabla \delta m + (Am + Bm^3 - h)\delta m] dV \\ & + \int_{(S)} \left[\frac{C}{\Lambda} m - h_s \right] \delta m dS. \end{aligned} \quad (2.4)$$

The first term in the volume integral may be rewritten as

$$C \nabla m \cdot \nabla \delta m = \nabla \cdot (C \delta m \nabla m) - C \nabla^2 m \delta m \quad (2.5)$$

and the contribution to (2.4) of the first term on the right can be transformed into a surface integral through Gauss theorem. Then

$$\begin{aligned} \delta F[m] = & \int_{(V)} [-C \nabla^2 m + Am + Bm^3 - h] \delta m dV \\ & + \int_{(S)} C \left[-\mathbf{n} \cdot \nabla m + \frac{m}{\Lambda} - \frac{h_s}{C} \right] \delta m dS \end{aligned} \quad (2.6)$$

where \mathbf{n} is a unit vector normal to the surface and pointing inside the system.

At equilibrium the first order variation of the free energy vanishes. The volume part gives the Ginzburg-Landau equation

$$C \nabla^2 m(\mathbf{r}) = Am(\mathbf{r}) + Bm^3(\mathbf{r}) - h \quad (2.7)$$

governing the bulk equilibrium behaviour whereas the surface part provides the boundary condition

$$\mathbf{n} \cdot \nabla m(\mathbf{r}) = \frac{m(\mathbf{r})}{\Lambda} - \frac{h_s}{C}. \quad (2.8)$$

In the bulk the l.h.s. in (2.7) vanishes and the zero-field magnetization is given by

$$m_b = \begin{cases} (-A/B)^{1/2} \sim t^{1/2} & T \leq T_c \\ 0 & T > T_c \end{cases} \quad (2.9)$$

where $t \sim |A|$ is the reduced temperature. The spontaneous magnetization vanishes at T_c as a power of the reduced temperature with a mean field bulk exponent $\beta = 1/2$.

The connected part of the order parameter correlation function

$$\langle m(\mathbf{r})m(\mathbf{r}') \rangle_c = \langle m(\mathbf{r})m(\mathbf{r}') \rangle - \langle m(\mathbf{r}) \rangle \langle m(\mathbf{r}') \rangle = \frac{\delta m(\mathbf{r})}{\delta h(\mathbf{r}')} \quad (2.10)$$

can be obtained through the introduction of a varying bulk external field $h(\mathbf{r})$ in (2.2). This simply amounts to replacing h in (2.7) by $h(\mathbf{r})$. Taking a derivative with respect to $h(\mathbf{r}')$ and using the definition (2.10) leads to

$$[-C\nabla_r^2 + A + 3Bm^2(\mathbf{r})] \langle m(\mathbf{r})m(\mathbf{r}') \rangle_c = \delta(\mathbf{r} - \mathbf{r}'). \quad (2.11)$$

For constant $m(\mathbf{r})$, which is the case in a homogeneous system below T_c or generally above T_c , the correlation function is therefore proportional to the Green function which satisfies

$$\left(-\nabla_r^2 + \frac{1}{\xi^2}\right) G(\mathbf{r}, \mathbf{r}') = \delta(\mathbf{r} - \mathbf{r}'). \quad (2.12)$$

Here

$$\xi = \begin{cases} \sqrt{\frac{C}{A}} & T > T_c \\ \sqrt{-\frac{C}{2A}} & T < T_c \end{cases} \quad (2.13)$$

is the bulk correlation length diverging at the critical point with a mean field exponent $\nu = 1/2$ which is the same in both phases. Hence the critical G is the Green function of the Laplace equation which establishes a link to electrostatic problems.

For a flat surface at $y = 0$ without external surface field, the boundary condition (2.8) gives

$$\frac{dm}{dy} = \frac{m}{\Lambda}. \quad (2.14)$$

When the surface interactions are not larger than in the bulk, due to the missing couplings at the boundary, the magnetization always increases from the surface into the bulk and the extrapolation length is positive. The surface transition is then driven by the bulk and there is an ordinary surface transition at T_c . Since $\Lambda \ll \xi$ near the bulk critical point, the magnetization profile extrapolates to zero near the surface and one may use Dirichlet

boundary conditions, i.e. $m = 0$ on the surface, instead of (2.14). With $\hat{m} = m/m_b$ and $h = 0$, (2.7) and (2.9) lead to

$$\frac{d^2 \hat{m}}{dy^2} = \frac{A}{C} \hat{m} + \frac{B}{C} m_b^2 \hat{m}^3 = -\frac{A}{C} (\hat{m}^3 - \hat{m}). \quad (2.15)$$

Multiplying both sides by $2d\hat{m}/dy$ and integrating, one obtains

$$\frac{d\hat{m}}{dy} = \frac{1 - \hat{m}^2}{2\xi} \quad (2.16)$$

where the integration constant has been chosen to give a vanishing slope at infinity and the form of the correlation length in (2.13) has been used. The solution of (2.16) with $\hat{m} = 1$ at infinity then is

$$m(y) = m_b \tanh \frac{y}{2\xi}. \quad (2.17)$$

In the vicinity of the surface, $m \sim t y$, so that the magnetization grows linearly with the distance to the surface. Its temperature dependence is different from the bulk one and involves a new exponent $\beta_s = 1$ which is the mean field surface exponent at the ordinary transition.

The form of the correlation function for the ordinary transition is given by the solution of (2.12) which satisfies Dirichlet boundary conditions at the surface. To obtain this function for a half-space, one can start from a d -dimensional slab limited by two surfaces at $y = 0$ and $y = L$. With $\mathbf{r} - \mathbf{r}' = \mathbf{r}_{\parallel} + (y - y')\mathbf{n}$ and taking advantage of translational invariance in the $d-1$ transverse directions, one may rewrite $G(\mathbf{r}_{\parallel}, y, y')$ as a Fourier expansion with components $G_{\mathbf{k}}(y, y')$ satisfying

$$\left(-\frac{\partial^2}{\partial y^2} + \kappa^2 \right) G_{\mathbf{k}}(y, y') = \delta(y - y') \quad (2.18)$$

where $\kappa = \sqrt{k^2 + \xi^{-2}}$. The solution can be written as an eigenfunction expansion

$$G_{\mathbf{k}}(y, y') = \frac{2}{L} \sum_{n=1}^{\infty} \frac{\sin(n\pi y/L) \sin(n\pi y'/L)}{\kappa^2 + n^2 \pi^2 / L^2}. \quad (2.19)$$

For a semi-infinite system $L \rightarrow \infty$ and the sum over n can be replaced by an integral which is evaluated using the method of residues so that finally [15]

$$G(\mathbf{r}_{\parallel}, y, y') = \frac{1}{(2\pi)^{d-1}} \int d^{d-1}k \frac{e^{i\mathbf{k} \cdot \mathbf{r}_{\parallel}}}{2\kappa} \left[e^{-\kappa|y-y'|} - e^{-\kappa(y+y')} \right]. \quad (2.20)$$

The two parts of G are each correlation functions of the infinite system, one between \mathbf{r} and \mathbf{r}' and the other between \mathbf{r} and the image point of \mathbf{r}' relative to the boundary. At

the critical point they decay with power $(d - 2)$. From this the surface-bulk correlations follow by taking $r_{\parallel} = 0$, y' fixed and $y \gg y'$, leading to the asymptotic decay $G(y) \sim y^{-(x+x_s)} \sim y^{-(d-1)}$. Here x and x_s are the bulk and surface (ordinary) scaling dimensions of the magnetization (Appendix A.1). The bulk behaviour is obtained taking y and $y' \gg 1$ with $|y - y'| \gg 1$. Then the decay exponent is $2x = d - 2$ so that

$$x = \frac{d-2}{2} \quad x_s = \frac{d}{2} \quad (\text{ordinary transition}). \quad (2.21)$$

The scaling relations (A4, A7) $\beta = \nu x = 1/2$ and $\beta_s = \nu x_s = 1$ are satisfied by the mean field exponents at the upper critical dimension which, in this case, is $d_c = 4$.

Finally, consider the critical profile of the magnetization when its value at the surface is fixed at $m(0) = m_0$. It follows from (2.7) with $A = 0$ and $h = 0$ so that

$$\frac{d^2 m}{dy^2} = \frac{B}{C} m^3. \quad (2.22)$$

Following the same steps as above, the integration gives

$$m(y) = m_0 \left[1 + m_0 \left(\frac{B}{2C} \right)^{1/2} y \right]^{-1} \quad (2.23)$$

with the asymptotic behaviour

$$m(y) \sim y^{-1}. \quad (2.24)$$

The magnetization decays as a power of the distance to the surface, a behaviour which is also obtained beyond mean field theory as discussed in the next section.

If the surface couplings are sufficiently enhanced and/or a surface field is present, Λ becomes negative and the surface orders at a temperature which is higher than the bulk critical one. Then bulk ordering at T_c induces some singularity in the surface behaviour. The associated critical point is the extraordinary transition. Increasing Λ decreases the temperature of the surface transition until the surface and the extraordinary transition meet at the special transition. A detailed treatment can be found in references [4, 15].

2.2. Correlation functions and critical profiles

Conformal methods (Appendix A.2) can be used to make quite general statements about critical systems. They generalize, at the critical point, the covariance under global scale transformations which is at the basis of the renormalization group, by introducing local scale transformations with a varying dilatation factor $b(\mathbf{r})$. Such local dilatations are realized via conformal transformations. In any dimension the conformal group is

constructed by including the inversion $\mathbf{r}' = \mathbf{r}/r^2$ besides the usual uniform transformations: translation, rotation and dilatation.

Particularly useful in the study of surface properties is the special conformal transformation [18,16]

$$\frac{\mathbf{r}'}{r'^2} = \frac{\mathbf{r}}{r^2} + \mathbf{a} \quad (2.25)$$

which combines an inversion followed by a translation and a new inversion. A semi-infinite system with a flat surface containing the origin is invariant under such a transformation when the translation \mathbf{a} is parallel to the surface. Using an infinitesimal translation, covariance under this transformation determines the form of the critical correlation functions [18] and allows a determination of boundary induced profiles. Although the transformation works in any dimension, only the two-dimensional situation is discussed below.

Consider a critical system on a half-plane with a surface at $y = 0$. In Cartesian coordinates (2.25) translates into

$$x' = x + \epsilon(x^2 - y^2) \quad y' = y + 2\epsilon xy \quad (2.26)$$

where the infinitesimal translation is $\mathbf{a} = (-\epsilon, 0)$. Using complex notations, $z = x + iy$, (2.25) is rewritten as

$$z' = z + \epsilon z^2 \quad (2.27)$$

and the local dilatation factor is

$$b(x) = \left| \frac{dz}{dz'} \right| = 1 - 2\epsilon x. \quad (2.28)$$

Let $\psi(\mathbf{r})$ be some local operator (energy density, order parameter) with bulk scaling dimension x , i.e. transforming as $\psi(\mathbf{r}/b) = b^x \psi(\mathbf{r})$ under a global change of scale. Its two-point critical correlation function $G(x_1, x_2, y_1, y_2) = \langle \psi(x_1, y_1) \psi(x_2, y_2) \rangle$, which is a function of x_1 and x_2 through $u = x_1 - x_2$ due to translational invariance parallel to the surface, is transformed into

$$G(u', y'_1, y'_2) = b(x_1)^x b(x_2)^x G(u, y_1, y_2) \quad (2.29)$$

according to (A14) under (2.26). A first-order expansion in ϵ leads to the differential equation

$$(x_1^2 - x_2^2 - y_1^2 + y_2^2) \frac{\partial G}{\partial u} + 2x_1 y_1 \frac{\partial G}{\partial y_1} + 2x_2 y_2 \frac{\partial G}{\partial y_2} + 2x(x_1 + x_2) G = 0. \quad (2.30)$$

Since G depends on x_1, x_2 only through u , all the terms involving a factor $x_1 + x_2$ sum up to zero and one obtains two partial differential equations

$$\begin{aligned} u \frac{\partial G}{\partial u} + y_1 \frac{\partial G}{\partial y_1} + y_2 \frac{\partial G}{\partial y_2} + 2xG &= 0 \\ (y_2^2 - y_1^2) \frac{\partial G}{\partial u} + u \left(y_1 \frac{\partial G}{\partial y_1} - y_2 \frac{\partial G}{\partial y_2} \right) &= 0. \end{aligned} \quad (2.31)$$

The first one expresses the homogeneity of the correlation function

$$G\left(\frac{u}{b}, \frac{y_1}{b}, \frac{y_2}{b}\right) = b^{2x} G(u, y_1, y_2) \quad (2.32)$$

or, with $b = u$ and $\zeta_i = y_i/u$,

$$G(u, y_1, y_2) = u^{-2x} G(1, \zeta_1, \zeta_2) = (u^2 \zeta_1 \zeta_2)^{-x} \Xi(\zeta_1, \zeta_2). \quad (2.33)$$

Using this form, the second equation in (2.31) fixes the way spatial coordinates combine into a single scaling variable ρ in the scaling function $\Xi(\rho)$ so that, finally,

$$G(x_1 - x_2, y_1, y_2) = (y_1 y_2)^{-x} \Xi \left[\frac{y_1 y_2}{(x_1 - x_2)^2 + (y_1 - y_2)^2} \right]. \quad (2.34)$$

The behaviour of the scaling function for small or large values of the argument can be deduced from scaling considerations. For instance, with $y_1 = y_2$ fixed and $|x_1 - x_2| = |u| \rightarrow \infty$, the surface-surface correlations decay like $|u|^{-2x_s}$ where x_s is the surface scaling dimension of ψ . As a consequence

$$\Xi(\rho) \sim \rho^{x_s} \quad \rho \rightarrow 0. \quad (2.35)$$

In two dimensions the scaling function itself satisfies a certain differential equation following from conformal invariance and has been determined explicitly for the Ising, Potts and $O(N)$ models [18, 16, 19, 20].

The same method applies to the determination of critical profiles when $\psi(\mathbf{r})$ is some quantity with nonvanishing average at the bulk critical point of a semi-infinite system. This may be either the energy density with free or fixed boundary conditions or the order parameter with fixed boundary conditions. Since in two dimensions the surface is one-dimensional, an enhancement of surface interactions is not sufficient to maintain surface order at the bulk critical point. Therefore the boundary variables must be fixed in order to have a non-trivial order parameter profile.

Due to translational invariance parallel to the surface, the critical profile depends only on y . Following the same steps as above, a differential equation for $\langle \psi(y) \rangle$ is obtained, leading to the universal profile

$$\langle \psi(y) \rangle \sim y^{-x}. \quad (2.36)$$

That (2.36) follows from conformal invariance was already noticed in a different way in [21, 22]. This algebraic form was originally deduced from simple scaling considerations [23]. In any number of dimensions, $\langle \psi(r_\perp/b) \rangle = b^x \langle \psi(r_\perp) \rangle$ where r_\perp is the distance to the surface, so that with $b = r_\perp$,

$$\langle \psi(r_\perp) \rangle \sim r_\perp^{-x}. \quad (2.37)$$

When ψ is the order parameter, $x = \beta/\nu$ which is equal to 1 in mean field theory in agreement with Equation (2.24).

2.3. Surface exponents

Some heuristic arguments have been used [24] to obtain the values of surface exponents in arbitrary dimensions. They apply to the ordinary and extraordinary transitions for the energy density and to the extraordinary transition for the order parameter. In two dimensions the results are supported by independent conformal arguments.

Consider a system inside a cube with L^d interacting spins and free boundaries. Increasing the size of the system by δL through the addition of a surface layer, the partition function becomes

$$Z_{L+\delta L} = \text{Tr} \exp[-\beta(\mathcal{H} + \delta\mathcal{H})] = Z_L \langle \exp(-\beta\delta\mathcal{H}) \rangle_L \quad (2.38)$$

where $\delta\mathcal{H}$ is the energy change associated with the extra layer. To leading order in L the free energy

$$F_L = L^d f_b + O(L^{d-1}) \quad (2.39)$$

only involves the bulk free energy density f_b . Its variation under an infinitesimal change of the size is given by

$$\delta F_L = -\beta^{-1} \ln \langle \exp(-\beta\delta\mathcal{H}) \rangle_L \simeq \langle \delta\mathcal{H} \rangle_L \simeq dL^{d-1} f_b \delta L + O(L^{d-2}) \quad (2.40)$$

so that

$$\lim_{\delta L \rightarrow 0} \frac{\langle \delta\mathcal{H} \rangle_L}{dL^{d-1}\delta L} = f_b + O(L^{-1}) \quad (2.41)$$

and the surface energy density ε_s on the l.h.s. scales near the bulk critical point like the bulk free energy density

$$\varepsilon_s \sim t^{\nu x_s} \sim f_b \sim t^{2-\alpha}. \quad (2.42)$$

Thus its scaling dimension x_s at the ordinary transition is equal to the dimensionality of the system according to the Josephson hyperscaling relation (A2). The same argument applies to the magnetization and energy densities with fixed boundary conditions, i.e. at the extraordinary transition. Then

$$m_s \sim \varepsilon_s \sim t^{2-\alpha} \quad (2.43)$$

so that both scaling dimensions are equal to the dimension d of the system. For the surface energy operator at the ordinary transition, this result was first obtained by Dietrich and Diehl in the $O(N)$ model using renormalization group methods and the short-distance expansion [25].

In two dimensions, any analytic function $w(z)$ on the complex plane provides a conformal transformation with a local dilatation factor $b(z) = |dz/dw|$ (see Appendix A.2). Such a transformation can be used to deduce surface exponents starting from the half-space critical profile. Under the conformal mapping $w = L/\pi \operatorname{arcosh} z$ the half-plane $y > 0$ is transformed into the half-strip ($u > 0$, $0 < v < L$, $w = u + iv$). The dilatation factor is $b(z) = \pi/L \sqrt{\sinh^2(\pi u/L) + \sin^2(\pi v/L)}$ and $y = \sinh(\pi u/L) \sin(\pi v/L)$. The boundary-induced critical profile $\langle \psi(y) \rangle$ (2.36) which has a bulk scaling dimension x , then transforms into [22]

$$\begin{aligned} \langle \psi(u, v) \rangle &\sim b(z)^x y^{-x} \\ &\sim \left(\frac{\pi}{L}\right)^x \left[\sinh^{-2}\left(\frac{\pi u}{L}\right) + \sin^{-2}\left(\frac{\pi v}{L}\right) \right]^{x/2} \end{aligned} \quad (2.44)$$

in the half-strip. The profile in the new geometry can also be written as an expansion in terms of the eigenstates of the transfer operator $\mathcal{T} = \exp(-\mathcal{H})$ where \mathcal{H} is the strip Hamiltonian with appropriate boundary conditions (Appendix B.1). Then

$$\langle \psi(u, v) \rangle = \sum_n M_n \langle n | \psi(v) | 0 \rangle \exp[-(E_n - E_0)u] \quad (2.45)$$

where E_0 is the ground-state energy of \mathcal{H} and M_n selects the eigenstates $|n\rangle$ compatible with the boundary conditions at $u = 0$. The smallest gap corresponding to a nonvanishing matrix element gives the surface scaling dimension x_s of ψ as in (A23). Since the large- u expansion of the r.h.s. of (2.44) involves only powers of $\exp(-2\pi u/L)$ the gaps in (2.45)

are multiples of $2\pi/L$. Assuming that M_1 is non-vanishing, one may identify the surface scaling dimension as

$$x_s = 2 \quad (2.46)$$

in agreement with previous results in the special case $d=2$.

The considerations presented above suppose the existence of a non-vanishing profile at the critical point. As a consequence they cannot be applied to the case of the magnetization at the ordinary surface transition. As mentioned in the preceding section, other conformal techniques can be used, which completely determine the critical correlation functions in the semi-infinite geometry. From these, the ordinary surface exponents given in Table 2.1 for the q -state Potts model and the $O(N)$ model have been identified [18, 16].

q -state Potts model ($d = 2$)					
q	0	1	2	3	4
x_s	0	$\frac{1}{3}$	$\frac{1}{2}$	$\frac{2}{3}$	1
$O(N)$ model ($d = 2$)					
N	-2	-1	0	1	2
x_s	1	$\frac{13}{16}$	$\frac{5}{8}$	$\frac{1}{2}$	$\frac{1}{4}$

Table 2.1. Order parameter scaling dimension at the ordinary surface transition in the q -state Potts model and the $O(N)$ vector model.

3. Wedges, corners and cones

Systems in the form of a wedge show new features and their study gives new insight into the influence of geometry on critical behaviour. They were first investigated by Cardy [26] using mean field theory in various dimensions and an ϵ -expansion near $d = 4$. Subsequently the corner geometry in $d = 2$ was studied by accurate calculations, mainly on Ising models, and by conformal mapping. The main result is that the edge and corner exponents are functions of the opening angle θ of the wedge. The planar surface and its exponents can be viewed as a simple special case.

This non-universal behaviour can be related to the particular geometrical properties of a wedge, which does not contain a length parameter and thus is invariant under rescaling.

The opening angle is therefore a marginal variable in a renormalization transformation and may enter into the expressions for the exponents. The same will happen for all other scale-invariant figures like arbitrary pyramids or cones. Furthermore, the system does not have to fill the figure, it may just cover the surface. For such a situation there are even exact analytical results.

3.1. Mean field theory

Within a continuum approximation, in the mean-field approach one has to solve the same equations as in Section 2.1, but for a different geometry. The order parameter correlation function is proportional to the Green function (2.12) with Dirichlet boundary conditions for the ordinary transition. This function also appears in electrostatics [27] and in diffusion problems [28]. In the present context it was discussed by Cardy [26] for wedges in d dimensions.

For a wedge, one proceeds as for a slab and performs a Fourier transformation in the $d-2$ directions parallel to the edge. In the remaining directions one uses polar coordinates ρ, α where α is the azimuthal angle in the wedge ($0 \leq \alpha \leq \theta$). The Fourier components $G_{\mathbf{k}}$ then satisfy

$$\left(-\frac{\partial^2}{\partial \rho^2} - \frac{1}{\rho} \frac{\partial}{\partial \rho} - \frac{1}{\rho^2} \frac{\partial^2}{\partial \alpha^2} + \kappa^2\right) G_{\mathbf{k}}(\rho, \alpha; \rho', \alpha') = \frac{1}{\rho} \delta(\rho - \rho') \delta(\alpha - \alpha') \quad (3.1)$$

with κ defined below (2.18). The solution can be written as an eigenfunction expansion and takes the form

$$G_{\mathbf{k}}(\rho, \alpha; \rho', \alpha') = \frac{2}{\theta} \sum_{n=1}^{\infty} \int_0^{\infty} \frac{d\mu}{\kappa^2 + \mu^2} \mu J_{\nu}(\mu\rho) J_{\nu}(\mu\rho') \sin\left(\frac{n\pi\alpha}{\theta}\right) \sin\left(\frac{n\pi\alpha'}{\theta}\right) \quad (3.2)$$

where the J_{ν} are Bessel functions and $\nu = n\pi/\theta$. The continuous index μ is related to the infinite extent of the system in the ρ -direction. Using this expression one can find, for example, the critical correlations parallel to the edge. Their asymptotic behaviour is determined by the contributions of $n = 1$ and small μ . One obtains

$$G(\mathbf{r}, \mathbf{r}') \sim \frac{1}{|\mathbf{r} - \mathbf{r}'|^{2x_e}} \quad (3.3)$$

with the edge exponent

$$x_e(\theta) = \frac{d-2}{2} + \frac{\pi}{\theta}. \quad (3.4)$$

The decay thus is always faster than in a homogeneous system, where it would be given by the first term in (3.4) as found in (2.21). This is an effect of the boundary conditions.

In an electrostatic picture, G gives the potential at \mathbf{r} due to a point charge at \mathbf{r}' and the effect comes from the induced charge of opposite sign on the (metallic) boundaries. For $\theta = \pi/n$, where n is an integer, it can be simulated by $(2n - 1)$ image charges. As the wedge becomes narrower, the effect becomes stronger.

To obtain the order parameter profile in the wedge one would have to solve the non-linear Ginzburg-Landau equation (2.7) with $h = 0$. For the critical behaviour, however, this is not necessary. The radial dependence has the general scaling form $m_b f(\rho/\xi)$ and since m is small, the spatial dependence follows from the linearized equation. This gives, for $\rho \ll \xi$

$$m(\rho, \alpha) \sim m_b \left(\frac{\rho}{\xi} \right)^{\pi/\theta} \sin \left(\frac{\pi\alpha}{\theta} \right) \quad (3.5)$$

Inserting the temperature dependence of ξ and m_b then leads to the exponent

$$\beta_e(\theta) = \frac{1}{2} \left(1 + \frac{\pi}{\theta} \right). \quad (3.6)$$

This result is valid in all dimensions. At the upper critical dimension $d_c = 4$ the scaling law $\beta_e = \nu x_e$ as in (A7) is satisfied although β_e and x_e are non-universal. For $\theta = \pi$ the surface exponent $\beta_s = 1$ is recovered. For smaller angles, the order parameter near the edge vanishes with zero slope at the critical temperature. This reflects the difficulty to maintain the ordered state in such a geometry.

One can also treat a semi-infinite wedge where the third planar boundary is perpendicular to the edge. This system has a three-dimensional corner with two right angles and the third one equal to θ . The correlation function then follows from the image method as

$$G(\mathbf{r}, \mathbf{r}') = G_\infty(\mathbf{r}, \mathbf{r}') - G_\infty(\mathbf{r}, \mathbf{r}'') \quad (3.7)$$

where G_∞ is the result for the infinite wedge and \mathbf{r}'' is the image point of \mathbf{r}' with respect to the third plane. For \mathbf{r}' near the corner, the correlations parallel to the edge then decay with a power $x_c + x_e = 1 + 2x_e$, from which the corner exponent $x_c(\theta) = 1 + x_e(\theta)$ follows. If $\theta = \pi/2$, one obtains a cubic corner with three right angles and $x_c = 7/2$. The exponent of the order parameter is calculated as above

$$\beta_c(\theta) = 1 + \frac{\pi}{2\theta}. \quad (3.8)$$

For small θ this is the same law as in (3.6) but in general $\beta_c > \beta_e$ so that the order near the corner vanishes faster with temperature than near the edge. In particular for the cubic corner one has $\beta_c = 2$, i.e. a quadratic behaviour.

The general three-dimensional corner, for which the exponents depend on three angles, has not been treated. However, results can be given for a cylindrical cone of opening angle θ with respect to the axis. The Green function of this problem has been determined in other contexts [28, 29]. For \mathbf{r}' on the axis and $r > r'$ it has the form

$$G(\mathbf{r}, \mathbf{r}') = \sum_{\mu} A_{\mu} \left(\frac{r'}{r} \right)^{\mu+1} P_{\mu}(\cos \alpha) \quad (3.9)$$

where again $0 \leq \alpha \leq \theta$. The Legendre function $P_{\mu}(\cos \alpha)$ has to vanish on the boundary ($\alpha = \theta$) which determines the allowed values $\mu = \mu_m$, $m = 1, 2, \dots$. The asymptotic decay is again a power law with the exponent given by the smallest $\mu_1 = \mu_1(\theta)$. For the order parameter near the apex of the cone one obtains, in the same way as for the wedge

$$\beta_a(\theta) = \frac{1}{2}[1 + \mu_1(\theta)]. \quad (3.10)$$

The function $\mu_1(\theta)$ is shown in reference [30]. For $\theta \rightarrow 0$ it varies as $1/\theta$ and the system has the same features as a narrow wedge. For $\theta = \pi/2$ one has $\mu_1 = 1$ and the result $\beta_a = \beta_s = 1$ for the planar surface is recovered. For $\theta \rightarrow \pi$ the quantity μ_1 vanishes logarithmically. Thus one obtains the bulk result $\beta_a = \beta = 1/2$, although one is dealing with a system from which an half-infinite needle is cut out.

3.2. Ising models

A number of results exist for corners in two-dimensional Ising lattices with certain discrete values of the angle. The corner magnetization m_c has been calculated for triangular and square lattices in three different ways : from star-triangle recursion equations [31], from the corner-corner correlation function [31–33] and from Baxter's corner transfer matrix [34].

In the recursion method, one starts from a finite lattice, e.g. in the shape of a triangle with fixed spins along one edge, and reduces it successively to smaller sizes. In this way the corner magnetization can be evaluated exactly, but the procedure has to be done numerically. In the second method one considers the correlation between spins at adjacent corners of a lattice in the form of a square. Asymptotically, it factors into the product of the two corner magnetizations for which an expression

$$m_c \sim \frac{\langle 1 | \sigma_1^x | B \rangle}{\langle 0 | B \rangle} \quad (3.11)$$

is found. Here the operator σ_1^x refers to the corner spin, the states $|0\rangle$ and $|1\rangle$ are the eigenstates of the row transfer matrix (Appendix B.1) with largest and next-largest

eigenvalue, and $|B\rangle$ describes the state of free spins in the upper and lower boundary row. The quantity m_c can then be determined from the solution of a matrix or integral equation. The corner transfer matrix, finally, is already the partition function for a whole angular segment (see Appendix B.2). Thus it is, from a geometrical point of view, the ideal tool for treating the corner geometry. However, due to the edges of free spins one has to take a matrix element $\langle B|\mathcal{T}|B\rangle$ and the calculation becomes relatively difficult. One has to solve a matrix equation also in this case.

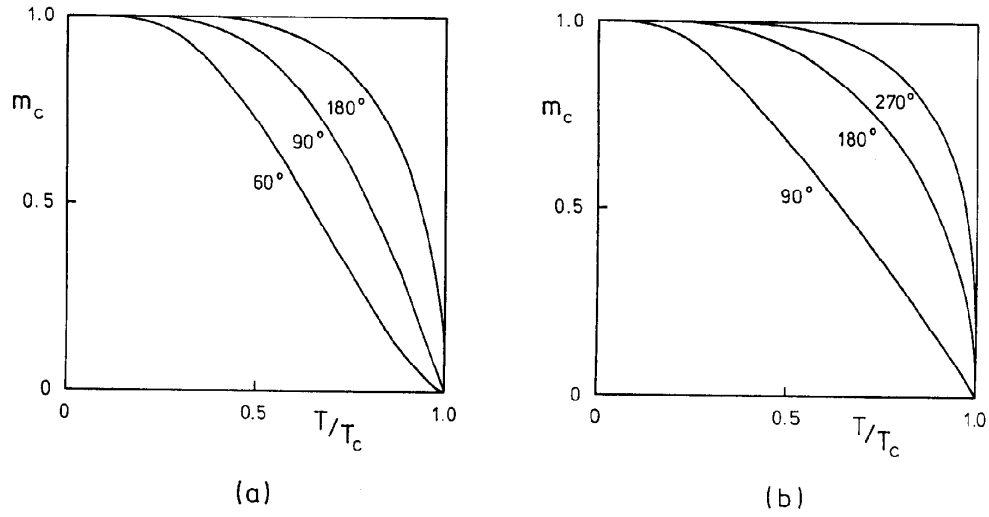


Figure 3.1. Corner magnetization vs. temperature for isotropic Ising lattices with various opening angles. Except for the 60° case all results refer to square lattices. (a) edges along the bonds (b) edges along the diagonals.

In Figure 3.1 results are shown for isotropic systems with various opening angles at the corner. The basic feature is that m_c decreases with decreasing θ for all non-zero temperatures. There is no general explicit result for $m_c(t, \theta)$ because even the transfer matrix calculations involve some numerics in the end. Based on the numerical results there is, however, a conjecture for a square lattice with a 90° corner and edges along the bonds [33]

$$m_c = 1 - \frac{1}{2}(\coth K_1 - 1)(\coth K_2 - 1) \quad (3.12)$$

where K_1, K_2 are the couplings in the two directions. The orientation of the edges and the precise location of the chosen spin both affect m_c [32] but not the critical exponent for which the formula

$$\beta_c = \frac{\pi}{2\theta} \quad (3.13)$$

was inferred from the data for isotropic systems with discrete angles [31]. Since $\nu = 1$ here, this is also the result for x_c . Thus one finds a simple $1/\theta$ -dependence on the angle as in the mean field treatment. If the system is anisotropic equation (3.13) is not immediately valid. However, by a rescaling as in Appendix B.1, one can make the system effectively isotropic. The opening angle θ thereby changes to an effective angle θ_{eff} , as illustrated in Figure B2, which need not be a simple fraction of π . With the new angle, equation (3.13) is again satisfied. It was shown later that this θ -dependence is a consequence of conformal invariance (see Section 3.4).

Ising models covering the surface of a pyramid have also been treated [31]. They are obtained by putting together k lattice segments, each with opening angle α , so that $\theta = k\alpha \neq 2\pi$. The calculation in this case is much simpler since the system is closed upon itself and has no edges of free spins. One can then use corner transfer matrices and derive the apex magnetization m_a from a simple trace formula, see (B18–19). The result takes the form

$$m_a(t, \theta) = \prod_{l=1}^{\infty} \tanh \left[(2l-1) \varepsilon(t) \frac{\theta}{2\pi} \right] \quad (3.14)$$

where $\varepsilon(t) \sim 1/\ln(1/t)$ for $t \rightarrow 0$. Curves for $m_a(t)$ look qualitatively similar to those shown in Figure 3.1. The critical behaviour can be found by converting the product in (3.14) into the exponential of an integral. The logarithmic dependence of ε on t then leads to a power-law behaviour of m_a . From the way the angle θ enters it follows that the apex exponent $\beta_a = x_a$ is related to the bulk value via

$$\beta_a = \frac{2\pi}{\theta} \beta. \quad (3.15)$$

This result also follows from conformal invariance. For a finite system at the bulk critical point, the variable t^{-1} in ε , which is proportional to the correlation length, is replaced by the size L [35] so that m_a varies as L^{-x_a} as in (A8).

3.3. Other systems

The corner geometry has also been investigated for the $O(N)$ -model in the limit $N \rightarrow 0$. In this case the spin correlation function is related to self-avoiding walks (SAW's) on the underlying lattice via [36]

$$G(\mathbf{r}, \mathbf{r}') = \sum_{N=0}^{\infty} K^N W_N(\mathbf{r}, \mathbf{r}') \quad (3.16)$$

where K is the coupling constant of the vector model and $W_N(\mathbf{r}, \mathbf{r}')$ denotes the number of SAW's with N steps, going from \mathbf{r} to \mathbf{r}' . By counting walks up to $N \sim 25$ for several angles, Guttman and Torrie [37] found in two dimensions

$$x_c = \frac{5\pi}{8\theta}. \quad (3.17)$$

For wedges in three dimensions they found the edge index

$$x_e = 0.5 + 0.847 \frac{\pi}{\theta}. \quad (3.18)$$

So far this is the only result in $d = 3$ beyond mean field theory.

One can also go the other way and derive properties of W_N from those of G , invoking conformal invariance [38, 39]. This was also done for polymers in corners [40]. For the walks one obtains, for example, the spatial moments of W_N . These were studied for systems in $d = 2, 3$ with excluded half-infinite lines, which are special cases of corners and cones, respectively [41, 39].

3.4. Conformal results

In two dimensions the critical behaviour of a wedge can be related to that of a half-plane if the system shows conformal invariance. This is done through the conformal transformation $w = z^{\theta/\pi}$ [18, 31].

The critical correlation function $G(w, w')$ in the wedge is found by transforming (2.34) according to (A14). For w' near the corner and w far in the bulk, it varies as

$$G(w, w') \sim \frac{1}{|w|^{x+x_c}} \quad (3.19)$$

where x_c is given by

$$x_c = \frac{\pi}{\theta} x_s. \quad (3.20)$$

Thus the corner index is related to the surface index via the geometrical factor π/θ which also appears in the mapping. The results (3.13), (3.17) are special cases corresponding to the surface exponents $x_s = 1/2$ and $x_s = 5/8$ in the two models. This confirms that conformal invariance actually holds in these systems. By relating other exponents to x_c and repeating this for different scaling operators one can then derive the whole set of wedge indices.

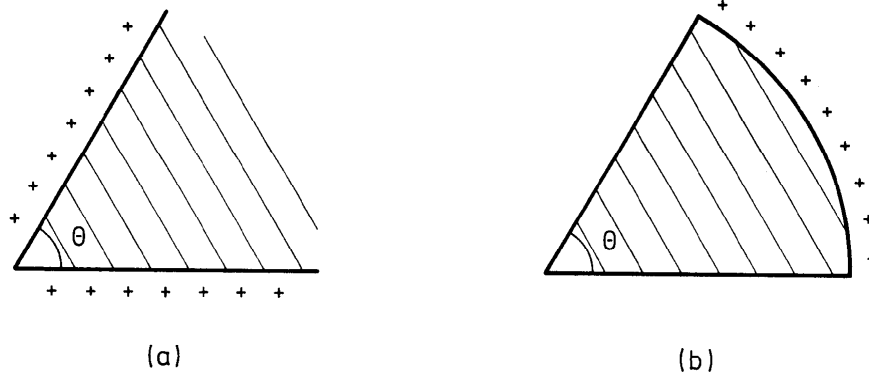


Figure 3.2. Two-dimensional corner geometry with two types of boundary conditions.

In the same way a conical system is obtained by mapping a full plane onto a wedge with periodic boundary conditions via $w = z^{\theta/2\pi}$. The correlation function in this geometry is then obtained from the one in the full plane via (A14). This leads to

$$x_a = \frac{2\pi}{\theta} x \quad (3.21)$$

relating apex and bulk indices, as already found in the treatment of the Ising model, cf. (3.15).

The mapping from the half-plane can also be used to determine the universal critical profiles, in the wedge geometry, which arise by fixing the variables along certain boundaries. Two situations are shown in Figure 3.2. For identical edges (Figure 3.2a) one finds [22]

$$\langle \phi(\rho, \alpha) \rangle \sim \left[\rho \sin \left(\frac{\pi \alpha}{\theta} \right) \right]^{-x} \quad 0 \leq \alpha \leq \theta. \quad (3.22)$$

If one of the edges is free, the surface index x_s also enters. In the half-plane this corresponds to a situation where one has free variables along half of the real axis and fixed ones along the other half. The profiles for such a case have so far only been determined for Ising and Potts models [42–44]. Taking these results one can also find the profiles for the case shown in Figure 3.2b. The necessary mapping is $w = \zeta^{\theta/\pi}$ with $\zeta = a(\sqrt{z} - 1)/(\sqrt{z} + 1)$. This transforms the upper z -plane onto a half-disc in the ζ -plane and onto a wedge with circular boundary of radius R in the w -plane. Near the corner, the result for the profile is

$$\langle \phi(\rho, \theta/2) \rangle \sim \frac{\rho^{x_c - x\pi/\theta}}{R^{x_c}} \quad \rho \ll R. \quad (3.23)$$

For the analogous conical system the profile only depends on ρ and follows from the result for a disc [22]. The size dependence is then given by R^{-x_a} .

With complex mapping one can also study rounded corners. In agreement with general predictions [5] one finds that the rounding does not affect the corner exponents or the asymptotic form of G in (3.19).

Conformal invariance also predicts universal contributions to the critical free energy which are connected with a corner or an apex [45]. For a finite two-dimensional system of characteristic size L , the free energy has the form

$$F = f_b L^2 + f_s L + \dots \quad (3.24)$$

where the terms written are the bulk and surface contributions, respectively. For systems with Euler number $\chi = 0$ like cylinders or tori, the next term is a universal constant, related to the Casimir effect [46, 47]. For $\chi \neq 0$, however, as is the case for simply connected domains, the next term is a logarithm in L . Each corner leads to a contribution

$$\Delta F_c = \frac{c\theta}{24\pi} \left[1 - \left(\frac{\pi}{\theta} \right)^2 \right] \ln L \quad (3.25)$$

where c is the conformal anomaly characterizing the universality class of the system. For the Gaussian model ($c = 1$) there is a close connection [48] between this term and the contribution of a corner to the eigenvalue spectrum of the Laplace operator as studied by Kac and others [49–51]. Thus the same geometrical factor appears in both cases. An apex of a cone gives an analogous contribution as (3.25), with the substitution $\pi/\theta \rightarrow 2\pi/\theta$ in the bracket.

Adding the contributions (3.25) for a system in the form of a rectangle gives $\Delta F = -(c/4) \ln L$. For the Gaussian model with fixed boundary variables this can be checked by a direct calculation [52, 53]. This result has been used to discuss the shape dependence of the critical free energy [54]. For a polygon with a large number of edges, ΔF approaches the result

$$\Delta F = -\frac{c\chi}{6} \ln L \quad (3.26)$$

valid for smooth boundary curves. Privman has given an interpretation of the logarithm in terms of an interplay of singular and non-singular contributions in the free energy [55]. According to this argument such terms can also arise from corners in three dimensions.

4. Parabolic shapes

A qualitative change in the critical behaviour occurs for systems which are asymptotically narrower than wedges or cones. This was observed in a study of two-dimensional systems bounded by algebraic curves of the form $v = \pm Cu^\alpha$ [56]. A typical case is the simple parabola ($\alpha = 1/2$) and, generally, such shapes will be called parabolic. The wedge corresponds to the special case $\alpha = 1$. Three typical situations are shown in Figure 4.1.

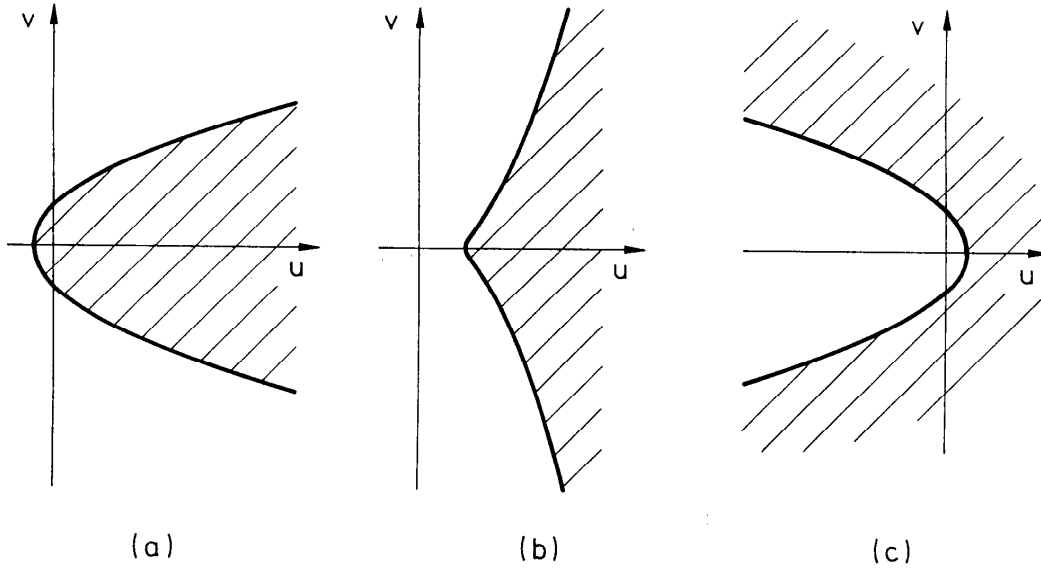


Figure 4.1. Three types of two-dimensional systems bounded by simple parabolic curves.

Using conformal and transfer matrix methods the following features were found. For $\alpha < 1$ the critical behaviour is no longer characterized by the usual power laws but by stretched exponentials. Thus thermodynamic quantities show essential singularities. Furthermore there is non-universality since the amount of stretching is determined by the value of α . For $\alpha > 1$, on the other hand, one finds normal surface critical behaviour. The difference between the two cases can be attributed to the way the dimensional parameter C behaves under renormalization for $\alpha < 1$ and $\alpha > 1$. The wedge geometry, $\alpha = 1$, is thereby seen to be the borderline case. A corresponding distinction holds in higher dimensions. For intrinsically anisotropic systems an analogous classification holds but the marginal case is then found for $\alpha \neq 1$.

4.1. Mean field theory

The simplest example is a two-dimensional system with parabolic boundary, $v^2 = 2pu + p^2$, as in Figure 4.1a. Its critical correlation function can be obtained by direct

calculation from (2.12) or using the transformation $z = i \cosh \pi \sqrt{w/2p}$ which maps the upper z -half-plane on the interior of a parabola in the w -plane. For points on the axis with u' fixed and u large, one finds

$$G(u, u') \sim \exp \left[-\pi \left(\frac{u}{2p} \right)^{1/2} \right]. \quad (4.1)$$

The decay of G is therefore faster than in a wedge, but slower than in a strip where G varies as $\exp(-\pi u/L)$, if the width is L . The power $u^{1/2}$ in (4.1) is clearly related to the form of the boundary. The length scale is set by the parabola parameter p or, equivalently, by the quantity $C = \sqrt{2p}$.

In three dimensions, a similar result is obtained for a paraboloid of revolution [57]. Working in parabolic coordinates, one can express G in terms of Bessel functions [58]. On the axis it has the form, for $u > u'$

$$G(u, u') = \sum_{m=1}^{\infty} A_m(u') K_0 \left[\mu_m \left(\frac{u}{2p} \right)^{1/2} \right] \quad (4.2)$$

where μ_m is the m -th zero of the Bessel function J_0 . Therefore asymptotically

$$G(u, u') \sim \frac{1}{u^{1/4}} \exp \left[-\mu_1 \left(\frac{u}{2p} \right)^{1/2} \right] \quad (4.3)$$

with $\mu_1 \simeq 2.41$. Here the power in front of the exponential is also related to the shape since it does not appear for a cylinder. As in Section 3.1, the result may be interpreted in electrostatic terms. The induced charge in the present case is more concentrated near the source point u' so that the decay of G is faster than in the conical geometry.

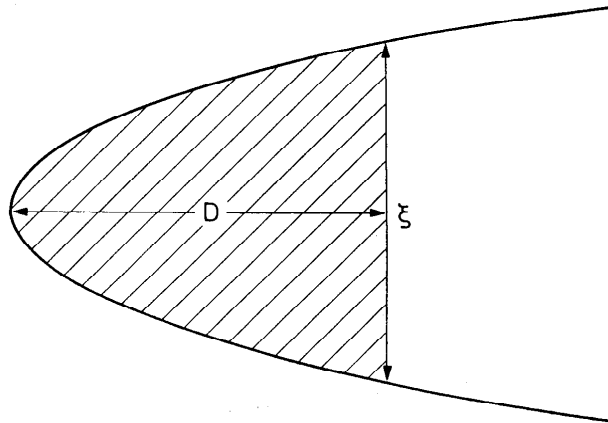


Figure 4.2. Geometry of parabolic system near the tip. The shaded portion of size D along the axis is the region where the shape governs the critical behaviour.

There exists no exact calculation of the order parameter $m(\mathbf{r})$ using (2.7). However, near the critical point one may integrate the linearized equation from the tip up to $u = D \sim \xi^2/p$, where the width of the system becomes comparable to ξ and $m(\mathbf{r})$ reaches its bulk value (Figure 4.2). In this region m increases exponentially in $(u/2p)^{1/2}$ and, for fixed u

$$m \sim \exp(-a\xi/p) \quad (4.4)$$

where a is a constant. The order therefore vanishes exponentially in $t^{-1/2}$ at T_c .

4.2. Conformal and scaling results

In two dimensions one can go beyond mean field theory and obtain results for arbitrary models which are conformally invariant. Complex mapping from the upper z -half-plane allows to obtain the three types of shapes shown in Figure 4.1. For $\alpha < 1$ (Figure 4.1a) it is given by $z = i \cosh(w/2p)^\alpha$. The critical correlation function is then found as in the case of a wedge. For points on the axis and large values of u [56]

$$G(u, u') = A(u') \frac{1}{u^{\alpha x}} \exp \left[-\frac{\pi x_s}{2C(1-\alpha)} u^{1-\alpha} \right]. \quad (4.5)$$

The functional form of G thus varies continuously with the parameter α . The fall-off is fastest for $\alpha = 0$ which corresponds to a semi-infinite strip of width $2C$. With increasing α the exponential becomes more and more stretched and approaches a power law for $\alpha \rightarrow 1$, the wedge limit. For $\alpha = 1/2$, the mean field (Gaussian) result (4.1) is reobtained by inserting the bulk and surface exponents $x = 0$, $x_s = 1$ (2.21). One also notes that the three-dimensional result (4.3) has the same structure as (4.5) and the power $1/4$ in (4.3) can be interpreted as αx , since $x = \frac{1}{2}$ is the mean field exponent in three dimensions.

By mapping the full z -plane one obtains systems with identical upper and lower boundaries ("paraboloids"). As in the passage from the wedge to the cone in Section 3.4, one then has to replace πx_s by $2\pi x$ in (4.5). For the Ising and Potts models one may also find, as in Section 3.4, the complete order parameter profile at the critical point if the variables are fixed at the right end of the system. The size dependence of the order parameter near the tip is then given, for both geometries, by the same exponential which appears in G , with u replaced by the size L .

For $\alpha > 1$ (Figure 4.1b) the mapping has to be changed into $z = i(w^s - p^s)^{1/s}$ where $s = (\alpha - 1)/\alpha$. Then on the axis, asymptotically,

$$G(u, u') \sim \frac{1}{u^{x+x_s}} \quad (4.6)$$

which is the result of the half-plane. Finally, if a parabolic piece with $\alpha < 1$ is cut out of an infinite system (Figure 4.1c) one obtains

$$G(u, u') \sim \frac{1}{u^{x+x_c}} \quad (4.7)$$

with the corner exponent $x_c(2\pi) = x_s/2$ for a cut (see (3.16)).

These results can be understood if one considers the behaviour of the boundary curves under a rescaling $\mathbf{r} \rightarrow \mathbf{r}' = \mathbf{r}/b$. Their functional form, being a power law, is invariant but the parameter C changes according to

$$C' = b^{\alpha-1}C. \quad (4.8)$$

For $\alpha > 1$, C grows under renormalization and the boundary approaches a straight line. For $\alpha = 1$, C is invariant and thus a marginal variable (the angle of Section 3). For $\alpha < 1$, C decreases and the system approaches either a cut geometry or becomes locally one-dimensional. In the latter case there is a destruction of long-range order which leads to the particular features found above. The same considerations hold for paraboloids in three dimensions. A parabolic cylinder, on the other hand, renormalizes to a half-plane in the latter case which has long-range order. This order, however, appears only at a lower temperature and stretched exponentials at the original transition are still possible.

The variable $1/C$ may be considered as a scaling field which plays the same rôle as the variable $1/L$ in finite-size scaling (Appendix A.1). It has dimension $1 - \alpha$ and vanishes at the fixed point of the half-plane geometry. It appears in scaling relations like the one for the magnetization on the axis (cf (A31))

$$m\left(t, u, \frac{1}{C}\right) = b^{-x} m\left(b^{1/\nu}t, \frac{u}{b}, \frac{b^{1-\alpha}}{C}\right) \quad (4.9)$$

leading to the functional form

$$m\left(t, u, \frac{1}{C}\right) = t^\beta g\left(\frac{u}{t^{-\nu}}, \frac{t^{-\nu(1-\alpha)}}{C}\right). \quad (4.10)$$

Assuming that, as in the mean field case, the tip magnetization is proportional to the critical correlation function between $u = 0$ and $u = D \sim (\xi/C)^{1/\alpha}$ (cf Figure 4.2), one obtains for $\alpha < 1$ from (4.5)

$$m(t) \sim \exp\left[-\frac{a}{(1-\alpha)}\left(\frac{t^{-\nu(1-\alpha)}}{C}\right)^{1/\alpha}\right]. \quad (4.11)$$

An essential singularity as encountered here has also been found in the six-vertex model [6] related to two-dimensional ice problems and to the roughening transition [59]. In this homogeneous system, however, all relevant quantities (free energy, correlation length and order parameter) vary in this way and the transition, which has been called of infinite order, is different from the present one.

4.3. Ising model

Calculations have been done to confirm in particular the behaviour (4.11) of the magnetization [56, 60]. For this the corner transfer matrix method was adapted to the parabolic geometry. Thus one works with the transfer matrix relating the spins along the upper and the lower boundary of the system. In the Hamiltonian limit this leads to an inhomogeneous quantum spin chain (Appendix B.2). If one deals with a lattice, the boundaries actually are step functions and the same then holds for the coefficients in the chain Hamiltonian (B3). Within a continuum interpolation they take the forms

$$h_n = (2n + \mu)^\alpha \quad \lambda_n = \lambda(2n + \nu)^\alpha \quad (4.12)$$

so that h_n and λ_n vary as n^α , reflecting the shape of the system. The parameters μ, ν allow for differences in the total number of vertical and horizontal bonds at position n . For the case $\alpha = 1/2$, $\mu = 0$, $\nu = 2$, the chain Hamiltonian can be diagonalized with the help of special polynomials [56]. For other cases the problem was studied numerically and via a continuum approximation [60]. It was found that, for $\alpha < 1$, the single particle eigenvalues ω_l vary as $(2l-1)/L^{1-\alpha}$ for a finite critical system and as $l^\alpha/\xi^{1-\alpha}$ near criticality, reflecting again the geometry. For a "paraboloid" the formula (B19) can then be used to obtain the magnetization at the tip. It reproduces the conformal prediction at criticality and gives

$$m \sim t^{-(1-\alpha)/2} \exp \left[-at^{-(1-\alpha)/\alpha} \right] \quad (4.13)$$

near the critical point. The exponential factor coincides with the expression (4.11) for $\nu = 1$. Formally, the exponential dependence appears, because the eigenvalues ω_l scale with a power of t in contrast to the case of a wedge where they vary logarithmically with t .

Calculations for the case of free boundaries have not yet been done with this method. However, the problem was studied via Monte Carlo simulations and the same typical behaviour of m was found [57]. One expects a different prefactor in this case but the data did not allow its determination. Physically, the exponential vanishing of m can be understood as follows: a system with $\alpha < 1$ is asymptotically narrower than any wedge

and so the magnetization close to the critical point should lie below an arbitrary power law.

4.4. Other systems

The previous considerations may be extended to systems displaying anisotropic critical behaviour. In this case the correlation lengths in two perpendicular directions diverge with different exponents ν_{\parallel} and ν_{\perp} . Then rescalings have to be performed with different factors $b_{\perp} = b$ and $b_{\parallel} = b^z$, where $z = \nu_{\parallel}/\nu_{\perp}$ [61]. Choosing the symmetry axis of the figure along the direction with ν_{\parallel} , the parameter C changes according to

$$C' = b^{z\alpha-1}C \quad (4.14)$$

and marginal behaviour occurs for $\alpha = 1/z$. Examples are provided by systems with uniaxial Lifschitz points [62], directed walks or directed polymers [63]. In the last two cases $z = 2$ and the borderline geometry is the normal parabola or, in three dimensions, the paraboloid. This situation was studied in [64, 65].

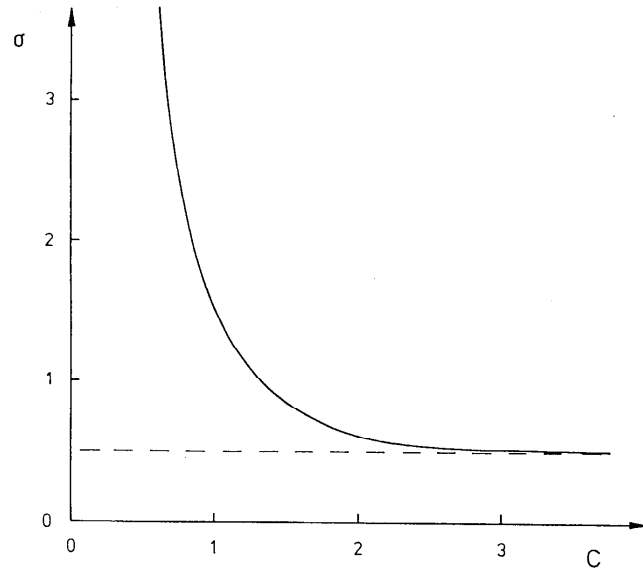


Figure 4.3. Exponent σ for the directed self-avoiding walk as a function of the parabola parameter C .

The simplest case is the directed self-avoiding walk in two dimensions. It is obtained by considering a usual one-dimensional random walk $x = x(t)$ as a path in the (x, t) -plane. In

the continuum limit, the relative number P of walks between two points (x, t) and (x', t') follows from the diffusion equation via

$$\left(\frac{\partial}{\partial t} - \frac{1}{2} \frac{\partial^2}{\partial x^2} \right) P(x, t | x', t') = \delta(x - x') \delta(t - t'). \quad (4.15)$$

This is the analogue of the Laplace equation for the critical mean field correlation functions considered before. At $x = \pm Ct^\alpha$ a time-dependent boundary condition is posed. In particular, if paths reaching the surface are terminated there, a necessary condition to obtain equal weights for all the walks with N steps in the original problem, one comes back to the Dirichlet boundary condition ($P = 0$) considered before.

In the marginal case $\alpha = 1/2$, if the paths start at the tip, the solution for large t is [64]

$$P(x, t | 0, 0) \sim \frac{1}{t^\sigma} F\left(\sigma, \frac{1}{2}; -\frac{x^2}{2t}\right). \quad (4.16)$$

The confluent hypergeometric function F has to vanish at the boundary, from which the exponent σ follows. It is shown in Figure 4.3. For $C \rightarrow \infty$ the usual Gaussian distribution with $\sigma = 1/2$ is reobtained. As C is lowered, the exponent σ increases monotonously, thus showing the expected non-universal behaviour. The decay of P with t thereby becomes faster in narrow systems, as found before for $z = 1$ in wedges and cones. Other exponents can be defined as usual. For example the survival probability, i.e. the relative number of walks reaching the time t (or having N steps in the discrete case) varies as $t^{\gamma_p - 1}$ with a susceptibility exponent $\gamma_p = 3/2 - \sigma$.

For the case $\alpha < 1/2$, the effect of the geometry is relevant and the form

$$P(x, t | 0, 0) \sim \frac{1}{t^\alpha} \exp\left(-\frac{\pi^2}{8C^2} \frac{t^{1-2\alpha}}{1-2\alpha}\right) \quad (4.17)$$

was deduced. It shows the same stretched exponential behaviour as the correlation functions in the previous sections. For $\alpha > 1/2$, the boundary is in a region where P is exponentially small anyway and therefore does not affect the behaviour in agreement with the scaling contained in (4.14). The results for the directed polymer problem, obtained on a discrete lattice via transfer matrix methods, are very similar [65].

Finally, normal SAW's with parabolic boundaries have been studied [66]. It was found that, for $\alpha < 1$, this originally isotropic system becomes anisotropic. A chain with N monomers then involves two radii of gyration: $R_{\parallel} \sim N^{\nu_{\parallel}}$ along the axis of the system and $R_{\perp} \sim N^{\nu_{\perp}}$ in the transverse direction. The chain configuration can be described using a blob picture [36] as shown in Figure 4.4. It results from the piling up of self-avoiding blobs inside the parabola. Within each blob the correlations are the same as in an unconfined

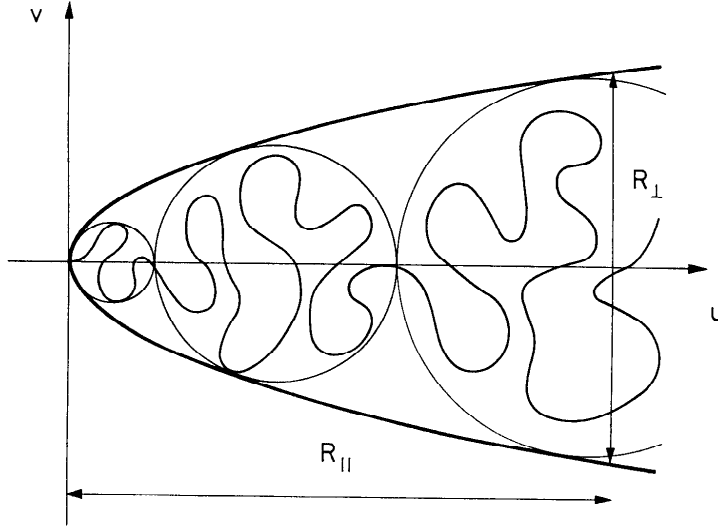


Figure 4.4. Blob picture for a polymer confined inside a parabola: the chain configuration results from the piling of self-avoiding fractal blobs (thin circles).

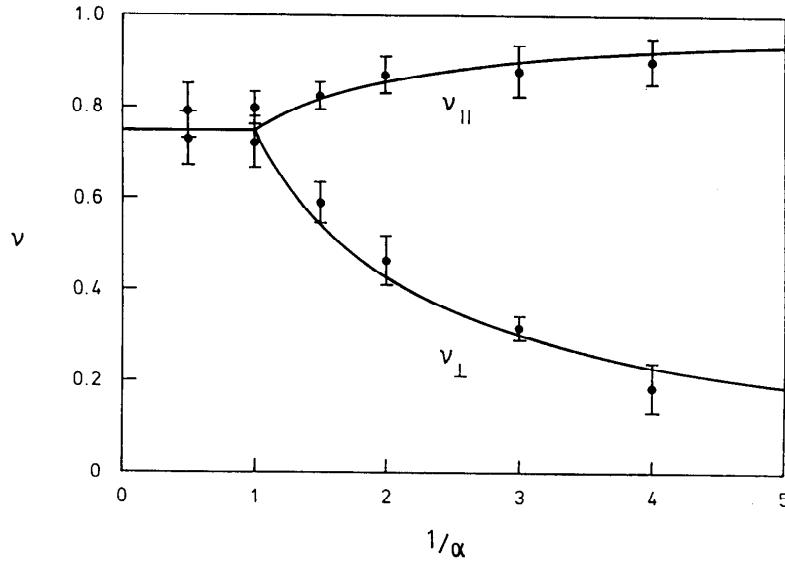


Figure 4.5. Variation with α^{-1} of the SAW exponents $\nu_{||}$ and ν_{\perp} in two dimensions for a chain confined inside a generalized parabola. The points are the results of Monte-Carlo simulations on a square lattice. The surface geometry is relevant and induces an exponent anisotropy when $\alpha < 1$.

chain. The radius R_{\perp} is given by the transverse size of the system at a distance $R_{||}$ from the tip so that $\nu_{\perp} = \alpha \nu_{||}$. This implies a new anisotropic fixed point for which, according to (4.14), the geometry remains invariant under renormalization since $z = 1/\alpha$. The evolution of the blob size along the axis of the system simply follows from the geometry and $R_{||}$ is

easily obtained as a function of N leading to

$$\nu_{\parallel} = \frac{\nu}{\alpha + \nu(1 - \alpha)} \quad (4.18)$$

where ν is the bulk exponent ($\nu = 3/4$ in $d = 2$). Monte-Carlo simulations on a square lattice (Figure 4.5) confirmed this picture and gave results compatible with (4.18). An accurate calculation of the correlation function like (4.16) has not yet been done.

5. Extended defects at surfaces

In the last sections, systems were treated where the geometry modifies the critical behaviour. We now turn to problems where a smoothly varying inhomogeneity in the couplings, decreasing from the surface, may influence the local critical properties. In real systems such an inhomogeneity could result from surface induced elastic deformations of the lattice. Thus one studies couplings which deviate from the bulk ones by an amount

$$\Delta K(y) = \frac{A}{y^{\omega}} \quad (5.1)$$

y being the distance from the surface.

Under a scale transformation $\mathbf{r}' = \mathbf{r}/b$ the coupling inhomogeneity, being an energy-like perturbation, transforms as $\Delta K'(y') = b^{1/\nu} \Delta K(y)$, therefore [67, 68]

$$A' = b^{1/\nu - \omega} A \quad (5.2)$$

where ν is the critical exponent of the correlation length. Thus, for $\omega > 1/\nu$, A decreases and one expects the same local critical behaviour as at a free surface. On the other hand, in the marginal case ($\omega = 1/\nu$) and in the relevant case ($\omega < 1/\nu$) scaling theory predicts local properties different from those of a simple free surface.

5.1. Ising model, general results

An extended defect of the form given in (5.1) was first studied by Hilhorst and van Leeuwen [69] in the two-dimensional Ising model. They considered the problem on a triangular lattice at the critical point. The nearest neighbour couplings $K_1(y)$ parallel to the surface and the diagonal ones $K_2(y)$ were different from their bulk values as in (5.1) with amplitudes such that $\Delta K_1(y)/\Delta K_2(y) = 2 \sinh(2K_1)/\cosh(2K_2)$.

The calculation of surface quantities was based on the repeated application of the star-triangle transformation [70] used also in calculations of the corner magnetization (Section 3.2). From the evolution of the couplings one can deduce the surface magnetization m_s

and the surface spin correlation function G_{\parallel} for any type of inhomogeneity in a numerical, iterative way. For smoothly varying perturbations as in (5.1), the asymptotic behaviour of the couplings after a large number of iterations and consequently the surface critical properties of the model can be determined exactly.

The results for the critical behaviour [69, 71, 72] are in complete agreement with the scaling arguments in the previous section. In detail they are:

i) For $\omega > 1/\nu = 1$, the perturbation is irrelevant, $m_s(t) \sim t^{1/2}$ and $G_{\parallel}(r) \sim r^{-1}$ as in the homogeneous, semi-infinite system.

ii) In the marginal case, $\omega = 1$, when A is smaller than a critical value $A_c > 0$, the decay of $G_{\parallel}(r)$ is non-universal with $2x_s = 1 - A/A_c$, while at $A = A_c$ where $x_s = 0$ the decay is logarithmic, $G_{\parallel}(r) \sim (\log r)^{-1}$. For strong enough enhancement of the couplings, $A > A_c$, there is a spontaneous surface magnetization at the bulk critical temperature. As A approaches A_c from above, it vanishes as $(A - A_c)^{1/2}$. The spin correlations in the surface approach their limiting value m_s^2 according to a power law with the non-universal exponent $2x_s = A/A_c - 1$.

iii) For $\omega < 1$ the perturbation is relevant. For any $A > 0$, there is a spontaneous surface magnetization at the bulk critical point which vanishes as $A^{1/[2(1-\omega)]}$ as A approaches zero. The correlation function G_{\parallel} has a stretched exponential form for any sign of A

$$G_{\parallel}(r) \sim \exp \left[-(r/\xi_{\parallel})^{1-\omega} \right] \quad \xi_{\parallel} \sim |A|^{-1/(1-\omega)}. \quad (5.3)$$

The problem was also studied on the square lattice using Pfaffian methods [73, 74]. In this case the couplings parallel to the surface were chosen to be constant $K_1(y) = K_1$, while the perpendicular ones were modified as in (5.1), writing

$$\Delta K_2(y) = \frac{\overline{A}}{y^{\omega}}, \quad \overline{A} = \frac{A}{4} \sinh(2K_2). \quad (5.4)$$

For the marginal problem ($\omega = 1$) the complete set of surface exponents, both those defined at the critical point and those associated with the approach to criticality, was determined. Furthermore, including a surface magnetic field h_s , the susceptibility exponents were also calculated. All exponents vary continuously with A . At the critical point the results are analogous to those obtained on the triangular lattice. The critical exponents have the same dependence on A/A_c in both cases. This is a kind of "weak universality" as observed also in other models containing a marginal operator [75].

The critical behaviour is anomalous in the regime of spontaneous surface order $A > A_c$. Then the scaling is anisotropic for $T > T_c$ and the local exponents are asymmetric, i.e. different for $T < T_c$ and $T > T_c$, respectively. This unusual behaviour can be explained

[76] assuming that the local energy density is a "dangerous irrelevant variable" [77] for $T > T_c$, whereas it is harmless in the region $T \leq T_c$.

5.2. Ising model boundary magnetization

For the Ising model on the square lattice, the surface magnetization at zero surface field is easily obtained using the transfer matrix method (Appendix B.1) [78, 79, 33]. It has been calculated first for the homogeneous system and later for inhomogeneous ones. The quantity m_s is deduced from the asymptotic value of the correlation function G_{\parallel} . In the anisotropic limit from (B11) it is found to be equal to the matrix-element of the operator σ_1^x between the ground state $|0\rangle$ and the first excited state $|1\rangle$ of the Hamiltonian in (B3)

$$m_s = \langle 1 | \sigma_1^x | 0 \rangle \quad (5.5)$$

In the general case, this has to be multiplied by $C_1 = \cosh K_1^*$ where K_1^* is the dual coupling defined below (B2). This expression holds in the low-temperature phase where the state $|1\rangle$ is degenerate with the ground state in the thermodynamic limit.

Using the fermion techniques described in Appendix B.1 one can express the matrix element by the surface component of the eigenvector Φ_s corresponding to the smallest excitation energy in (B8)

$$\langle 1 | \sigma_1^x | 0 \rangle = \Phi_s(1). \quad (5.6)$$

Since the vector Φ_s must be normalized, its component $\Phi_s(1)$ is only non-vanishing in the thermodynamic limit if the eigenstate is localized near the surface. Such a state, with a localization length diverging at the critical point, is known to exist below T_c [80, 78, 79].

Using (B8) and (B9) with $h_n = 1$, the surface magnetization of a very anisotropic, semi-infinite system can be expressed in closed form

$$m_s = \left[1 + \sum_{l=1}^{\infty} \prod_{n=1}^l \lambda_n^{-2} \right]^{-1/2} \quad (5.7)$$

Including a factor C_1 and putting

$$\lambda_n = \frac{\tanh K_2(n)}{\tanh K_1^*}. \quad (5.8)$$

the expression also holds outside the anisotropic limit. Close to the critical point, $\Phi_s(n)$ extends a long way into the bulk, therefore its normalization and thus m_s are determined

by its asymptotic behaviour for $n \gg 1$. For the couplings (5.4), in the extreme anisotropic limit, this gives

$$\lambda_n \simeq \lambda \left(1 + \frac{A}{2} n^{-\omega} \right) \quad (5.9)$$

where $\lambda = 1$ at the bulk critical point while $\lambda > 1$ and $\lambda < 1$ correspond to $T < T_c$ and $T > T_c$, respectively.

For the homogeneous model ($A = 0$) the sum in (5.7) is a geometric series. This gives $m_s = C_1(1 - \lambda^{-2})^{1/2}$ which is the result first found by McCoy and Wu [3]. Near the critical point $m_s \sim t^{1/2}$ so that the magnetic surface exponent is $\beta_s = 1/2$. For $\omega > 1$ the products in (5.7) are convergent, thus for large n the behaviour of $\Phi_s(n)$ is the same as for $A = 0$. As a consequence β_s remains unchanged and the perturbation is irrelevant. When $\omega < 1$, $\Phi_s(n)$ varies asymptotically as $\exp[-(A/2)n^{1-\omega}]$ corresponding to a localized state for $A > 0$. Then there is a spontaneous surface magnetization at the critical point which vanishes as $A^{1/[2(1-\omega)]}$ when A goes to zero, in accordance with results on the triangular lattice. For $A < 0$ on the other hand, there is no surface order at the critical point and m_s vanishes with an essential singularity according to

$$m_s \sim \exp \left[-\alpha(A, \omega) t^{-(1-\omega)/\omega} \right]. \quad (5.10)$$

In Figure 5.1 the temperature dependence of m_s is shown for an isotropic bulk system and various values of A .

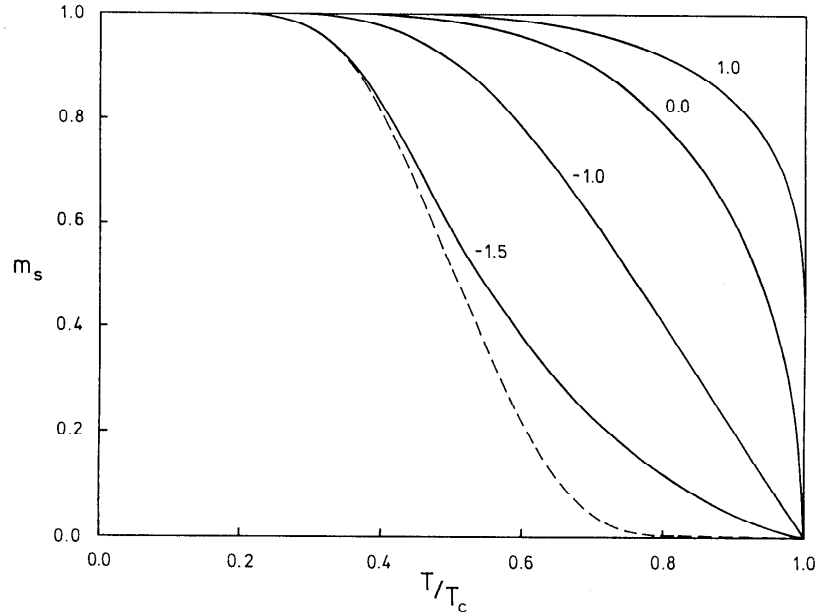


Figure 5.1. Boundary magnetization m_s vs. temperature in the Hilhorst-van Leeuwen model. The full lines correspond to $\omega=1$ and various values of A , the dashed line to $\omega=0.25$, $A=-1.5$.

In the marginal case $\omega = 1$, a closed form for m_s can be obtained if (5.9) is changed into $\lambda_n = \lambda(1 - A/2n)^{-1}$. Then

$$m_s = \left[F \left(1 - \frac{A}{2}, 1 - \frac{A}{2}; 1; \lambda^{-2} \right) \right]^{-1/2} \quad (5.11)$$

where $F(a, b; c; z)$ denotes the hypergeometric function [81]. Expanding (5.11) in powers of $t = 1 - \lambda^{-2}$ one obtains

$$m_s = \frac{\Gamma(1 - \frac{A}{2})}{\sqrt{\Gamma(1 - A)}} t^{(1-A)/2} \quad A < 1 \quad (5.12)$$

thus $\beta_s = (1 - A)/2$. Expressions for $A \geq 1$ can be obtained in the same way.

5.3. Conformal invariance for the marginal case

In section (2.2) it was shown that the special conformal transformation (2.26) which leaves the surface invariant can be used to obtain information on the critical behaviour. For the system considered here the geometry is the same and the inhomogeneity (5.1) transforms into itself in the marginal case $\omega = 1/\nu$ [82]. This suggests that conformal invariance holds in the same way as for the homogeneous case. In particular one can then map the half-space onto a strip as in (A22) and investigate the spectrum of the transfer matrix in this finite geometry. Under this mapping the inhomogeneity is transformed into a sinusoidal form [83]

$$\Delta K(u) = \overline{A} \left[\frac{L}{\pi} \sin \left(\frac{\pi u}{L} \right) \right]^{-\omega} \quad (5.13)$$

where L is the width of the strip and u , with $0 < u \leq L$, is the transverse coordinate. ΔK does not depend on the position along the strip.

For the Ising model, a strip with couplings given by (5.13) was studied at the bulk critical point by two different methods. The case of a triangular lattice was treated in [83] by a numerical method based on the star-triangle transformation [84]. For the square lattice, the spectrum of the transfer matrix was obtained analytically in the extreme anisotropic limit [83]. Thus the Hamiltonian H as in Appendix B.1 was investigated for couplings given by $h_n = 1$, $\lambda_n = 1 + \Delta K(n)/2$. The matrix equation (B8, B9) was transformed into a differential equation which is solved in terms of hypergeometric

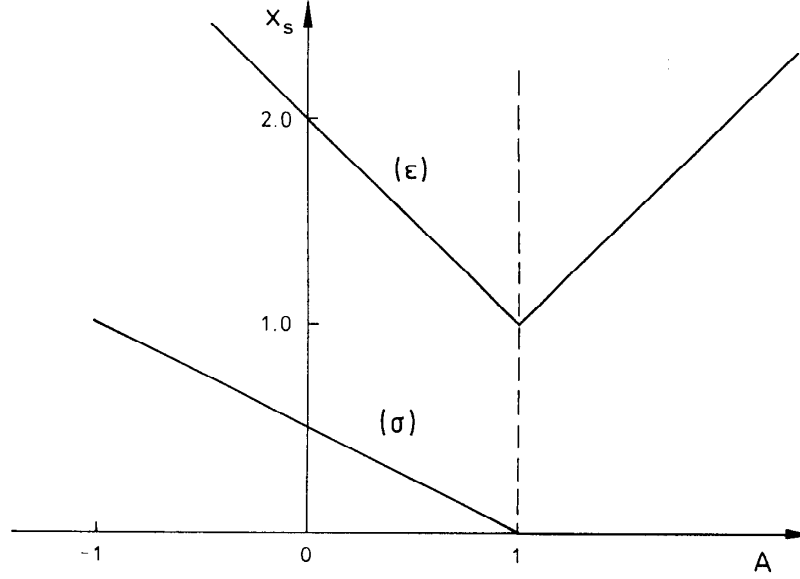


Figure 5.2. Surface scaling dimensions for spin (σ) and energy density (ε) in the Hilhorst-van Leeuwen model for $\omega=1$ as a function of the strength parameter A .

functions. In this way the lowest gaps, which are of order $1/L$, were determined in a continuum approximation as in [85].

The spectrum found in the second approach displays the tower-like structure typical of conformally invariant systems. From the lowest gaps surface exponents are deduced, using (A23), which are in agreement with those found from the calculations for the half-space [73, 74, 86]. They are shown in Figure 5.2 as functions of the parameter A . For $A > 1$ the lowest gap vanishes like L^{-A} , i.e. faster than $1/L$, in the large- L limit. Hence the smallest magnetic dimension vanishes. This is related to the fact that for $A > 1$ there is magnetic surface order at the bulk critical point. These scaling dimensions are also in agreement with the results of the first-order perturbation expansion (Table C2 in Appendix C), where, according to (5.4) and Appendix B.3, the defect amplitude becomes $g = A/4$ in the continuum limit. Similar conclusions are reached from the calculations on triangular lattices. These results strongly support the validity of conformal invariance for this particular inhomogeneous system. The correlation functions in the half-space therefore will have the same structure (2.34) as for a homogeneous system, but with a different scaling function.

5.4. Related problems

The Hilhorst-van Leeuwen model has been generalized recently by adding another marginal contribution with angular dependence to the inhomogeneity in (5.1). The

Hamiltonian spectrum in the associated strip was determined exactly, noticing the supersymmetric aspects of the eigenvalue problem [87].

For the most general marginal extended perturbation of the Ising model with the form $Af(\theta)/\rho^{1/\nu}$ in polar coordinates, the gap-exponent relation was shown to remain valid up to first order in the perturbation amplitude A [82].

In addition to the Ising model, the Gaussian model with a defect of the form (5.1) has also been studied [88]. This can be viewed as a mean field calculation which, however, is as complicated as the one for the Ising model. Using again the star-triangle transformation, the surface correlation function was determined as in Section 5.1. In the marginal case, which here corresponds to $\omega=2$, it decays with a non-universal exponent.

For systems with anisotropic scaling as described in Section 4.4, the relation (5.2) has to be used with the exponent ν in the direction of the inhomogeneity. For example, for a polymer directed along a surface and interacting with it, the monomer fugacity can be modified as in (5.1). Then one has $\nu_{\perp}=1/2$ in the transverse direction and the marginal case corresponds to $\omega=2$. For weak enough surface interaction ($A < A_c$), the polymer is free and can be characterized by critical exponents which depend on A . For stronger surface interaction, it becomes localized near the surface and the transition at $A=A_c$ is of infinite order [89].

The defects considered so far extended from the surface into the bulk. One may also consider perturbations which are confined to the surface but vary along it. For the Ising model the effect of an inhomogeneous field

$$h(x, y) = \frac{A}{|x|^{\omega}} \delta(y) \quad (5.14)$$

was studied in [90]. Under rescaling, the amplitude transforms as

$$A' = b^{1-x_s-\omega} A \quad (5.15)$$

where the scaling dimension of h_s in (A6) was used. For the Ising model, $x_s = 1/2$ (Table 2.1), which leads to marginal behaviour when $\omega = 1/2$. This also follows from Appendix C.2 with $d_{eff} = x_s$. Mapping the system onto a strip then leads to a homogeneous boundary field of strength $\sqrt{\pi/L}A$ which shifts the levels of the Hamiltonian by an amount of order $1/L$. The magnetic surface exponent determined via (A23) varies continuously between $x_l=x_s=1/2$ for $A=0$ and $x_l=2$ for $A \rightarrow \infty$. The latter case corresponds to fixed boundary conditions and is also realized when the perturbation is relevant. The correlation function decays towards a finite value in the strip and the exponent refers to the connected part.

A special form of inhomogeneity is present in quasiperiodic systems which interpolate between periodic and random systems and where the perturbation is spread over the whole volume. Results have recently been obtained for two-dimensional layered systems with quasiperiodic or aperiodic modulations. The relevance or irrelevance of the aperiodicity is connected to the strength of the fluctuations in the couplings [91] and the corresponding criterion is obtained [92] through a generalization of Harris's argumentation for random systems [93]. Exact results have been derived for the specific heat [91] and the surface magnetization [94, 92] for different aperiodic two-dimensional Ising models and their related quantum chains, as well as for directed polymers [92]. It was found that irrelevant aperiodicities indeed do not modify the critical behaviour, while for relevant perturbations the thermodynamic quantities show essential singularities at the critical point like in (5.10). As expected varying exponents are found in the marginal case.

5.5. Scaling considerations for relevant inhomogeneities

In the previous sections we have seen that the critical behaviour of different systems in the presence of relevant perturbations ($\omega < 1/\nu$) is very similar: critical correlations decay in a stretched exponential form, while the thermodynamic quantities have an essential singularity at the critical point. In the following we show how a general scaling theory together with plausible assumptions can explain these observations.

We start by considering the scaling behaviour of the surface magnetization

$$m_s(t, A) = b^{-x_s} m_s(b^{1/\nu} t, b^{1/\nu - \omega} A) \quad A > 0 \quad (5.16)$$

where we included the relevant scaling field A , with the transformation law in (5.2). Putting $b = \xi$ in (5.16) one obtains m_s in the form

$$m_s(t, A) = t^{\beta_s} f\left(\frac{l}{\xi}\right) \quad l = |A|^{-\nu/[1-\nu\omega]} \quad (5.17)$$

where l is a characteristic length introduced by the inhomogeneity which stays finite at the critical point. If m_s is to stay finite at bulk criticality the temperature dependence has to cancel. Then

$$m_s \sim A^{\nu x_s/[1-\nu\omega]} \quad A > 0. \quad (5.18)$$

For the Ising model this is the relation cited before in Section 5.1.

The scaling behaviour of the parallel correlation function is given by

$$G_{\parallel}(t, A, r) = b^{-2x_s} G_{\parallel}(b^{1/\nu} t, b^{1/\nu - \omega} A, \frac{r}{b}). \quad (5.19)$$

Taking $b=r$,

$$G_{\parallel}(t, A, r) = r^{-2x_s} g_{\parallel}(r^{1/\nu} t, r^{1/\nu-\omega} A) \quad (5.20)$$

where the scaling function in the homogeneous case ($A = 0$) behaves like $g_{\parallel}(u, 0) \sim \exp(-u^{\nu})$. To obtain information on the case $t = 0$, $A \neq 0$ consider the choice $\omega = 0$. Then one is dealing with an off-critical system where now A is playing the rôle of t . Therefore $g_{\parallel}(0, v) \sim \exp(-v^{\nu})$ in this case. Assuming that this also holds for $\omega \neq 0$ one arrives at

$$G_{\parallel}(r) \sim r^{-2x_s} \exp[-(r/l)^{1-\omega\nu}]. \quad (5.21)$$

for the critical correlations. This is the behaviour which was found in (5.3) for the Ising model [72]. A similar argument leads to the scaling form of the perpendicular correlation function at $t = 0$

$$G_{\perp}(r) \sim r^{-(x+x_s)} \exp[-(r/l)^{1-\omega\nu}]. \quad (5.22)$$

For reduced surface couplings ($A < 0$) the surface order, below the bulk critical temperature, is induced by the bulk magnetization at a distance D from the surface. The size of this surface region can be estimated by equating the thermal and inhomogeneity energy contributions, $t \sim |A|/D^{\omega}$. One may then argue as in Section 4.2 and assume that the order parameter near the surface is proportional to the correlation function $G_{\parallel}(r)$ with $r = D \sim (|A|/t)^{1/\omega}$ so that

$$m_s(t, A) \sim \exp\left[-a|A|^{1/\omega} t^{\nu-1/\omega}\right] \quad A < 0. \quad (5.23)$$

This is consistent with the Ising model result (5.10).

The results (5.21–23) have the same functional form as (4.5) and (4.11) for the parabolic geometry with the correspondence $\alpha \leftrightarrow \omega\nu$, $1/C \leftrightarrow |A|^{\nu}$. This can be understood as follows: in both problems, a position-dependent, smoothly varying local length-scale can be defined near T_c . For the parabola, it is proportional to the local width

$$\xi(x) = Cx^{\alpha} \quad (5.24)$$

while for an extended defect, since $\Delta K(y)$ is a local temperature shift

$$\xi(y) = \Delta K(y)^{-\nu}. \quad (5.25)$$

For the calculation of a correlation function between boundary and bulk variables, one can imagine the system divided into sections, so that in each of them there is a decay with the local length $\xi(x)$ or $\xi(y)$. The complete correlation function is then obtained in the form of a product, or equivalently, as

$$G_{\perp}(y_1, y_2) \sim \exp\left(-\int_{y_1}^{y_2} \frac{dy}{\xi(y)}\right). \quad (5.26)$$

Inserting for instance the form (5.25) then gives

$$G_{\perp}(y_1, y_2) \sim \exp\left[-a(y_2^{1-\omega\nu} - y_1^{1-\omega\nu})\right] \quad (5.27)$$

which corresponds to (5.22).

6. Narrow line defects in the bulk

In the last section the effects of extended defects at surfaces were treated. Narrow defects, where the couplings at the surface are modified only in a few layers do not change the critical behaviour in two dimensions. If the couplings are modified along a line, at a finite distance from the surface, a singularity in the surface correlation length appears below the bulk critical temperature [95]. This singular behaviour, however, occurs for a finite value of the correlation length and is not linked with any new fixed point. However, if defect lines are situated in the bulk, a rich local critical behaviour can be found. In this section we consider this situation with an emphasis on line and star defects.

First some mean field and scaling considerations are presented, which show how the dimensionalities of system and defect, the bulk and the surface scaling dimensions may affect the local critical behaviour. This is followed by a discussion of line and star defects in the two-dimensional Ising model for which exact results have been obtained, either directly in the plane geometry or, using a conformal mapping, in the strip geometry.

6.1. Mean field theory and scaling

In mean field theory the problem can be discussed for arbitrary dimension d . Assume that the system contains a defect of dimension d^* (a point, a line or a plane) so that the order parameter depends only on one coordinate r . Then the Ginzburg-Landau equation in the ordered phase reads in terms of reduced variables $\hat{m} = m/m_b$, $\hat{r} = r/\xi$ [96, 97]

$$\hat{r}^{-d+d^*+1} \frac{d}{d\hat{r}} \left(\hat{r}^{d-d^*-1} \frac{d\hat{m}}{d\hat{r}} \right) = \hat{m}^3 - \hat{m}. \quad (6.1)$$

The spontaneous magnetization takes the scaling form

$$m(r) = m_b f\left(\frac{r}{\xi}\right) \quad (6.2)$$

as in (2.17) for the free surface. Equation (6.1) has to be supplemented by boundary conditions. If the defect interactions are weaker than bulk ones, the extrapolation length discussed below (2.3) is positive and one may look for the conditions under which a solution exists which satisfies Dirichlet boundary conditions at the defect. Since $\hat{m} \ll 1$ near the defect, the local behaviour can be deduced from a linearized equation

$$\frac{d^2 \hat{m}}{d\hat{r}^2} + \frac{d-d^*-1}{\hat{r}} \frac{d\hat{m}}{d\hat{r}} + \hat{m} = 0 \quad (6.3)$$

which is of the Bessel type. An acceptable solution is obtained only when $d - d^* < 2$. It takes the form $\hat{r}^\mu J_\mu(\hat{r})$ with $2\mu = 2 - d + d^*$ and behaves like $\hat{r}^{2\mu}$ for small \hat{r} so that, near the defect

$$m(r) \sim r^{2-d+d^*} t^{(3-d+d^*)/2} \quad d - d^* < 2 \quad (6.4)$$

The perturbation is then relevant: the defect changes the local critical behaviour and leads to a magnetization exponent $\beta_l = (3 - d + d^*)/2$. For $d^* = d - 1$ one recovers the ordinary surface behaviour with $\beta_l = \beta_s = 1$. If $d - d^* > 2$ the perturbation should be irrelevant and one expects bulk critical behaviour. This can be shown using scaling arguments as follows. The coupling perturbation which belongs to the defect subspace of dimension d^* and couples to the bulk energy density ε with dimension $x = d - 1/\nu$ has a scaling dimension

$$d^* - x = d^* - d + \frac{1}{\nu} \quad (6.5)$$

As a result the perturbation is relevant (irrelevant) when $d - d^* < 1/\nu$ ($> 1/\nu$). With the mean field value $\nu = 1/2$, one finds the condition cited above.

If $d^* = d - 1$, the defect divides the system into two parts. Then if $\nu < 1$ and the local interactions are weaker than in the bulk, according to (6.5) the defect is expected to behave in the same way as a cut. Thus ordinary surface critical behaviour will result [15] provided the corresponding surface fixed point remains stable against a weak coupling between the surfaces of the two half-spaces. The condition for this can be found in the following way: starting from two free surfaces the perturbation involves the product of two surface magnetization operators with scaling dimension x_s and the dimension of the coupling is given by

$$d - 1 - 2x_s = \frac{\gamma_s}{\nu} \quad (6.6)$$

where γ_s is the local susceptibility exponent at the ordinary surface transition (A9). The system with the defect behaves in the same way as one with a free surface if this exponent is negative and $\nu < 1$ [98]. Non-universal local critical behaviour is expected when the perturbation is marginal, i.e. when $\nu = 1$ and $\gamma_s = 0$. These scaling results have been confirmed in a series of calculations on the $O(N)$ model in the limit $N \rightarrow \infty$ and using either ϵ - or $1/N$ -expansions [99–107].

6.2. Ising model with a defect line

According to the scaling arguments of the preceding section a defect line in the two-dimensional Ising model, which has exponents $\nu = 1$ and $\gamma_s = 0$ at the ordinary transition, is expected to lead to continuously varying local exponents. This problem was first

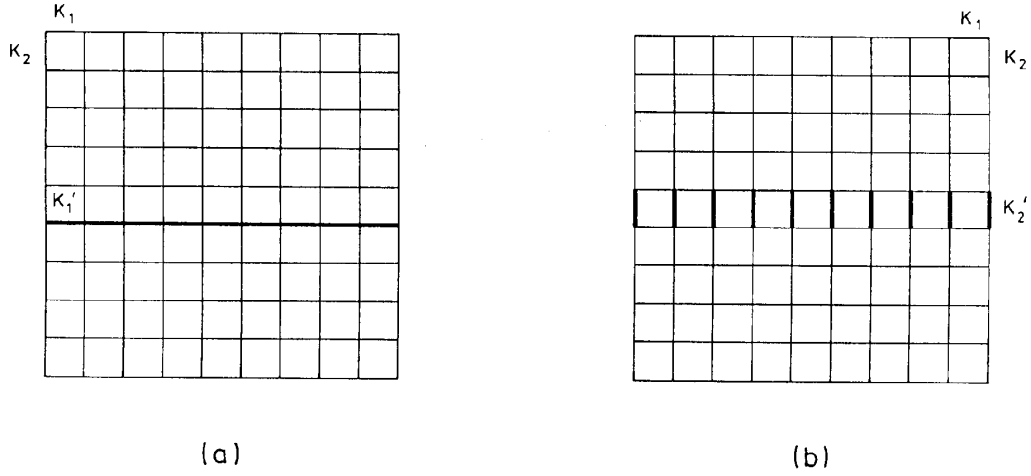


Figure 6.1. Ising square lattice with two kinds of defect lines (a) chain defect, (b) ladder defect.

investigated by Bariev [108] who deduced the local magnetization, as a function of the perturbation strength and distance to the defect, from the asymptotic behaviour of the two-spin correlation function below the critical temperature. This was followed by a detailed study of the two-spin correlation function by McCoy and Perk [109].

In the square lattice Ising model one can distinguish two types of perturbation as shown in Figure 6.1. The chain perturbation has modified couplings K'_1 parallel to the defect line whereas, for the ladder defect, perturbed couplings K'_2 are in the perpendicular direction. The local magnetization was found to vary as [108]

$$\langle \sigma(y) \rangle \sim t^{\beta_l} y^{\beta_l - \beta} \quad (6.7)$$

when the distance y to the defect line is much smaller than the bulk correlation length ξ . In this expression $\beta = 1/8$ is the bulk magnetization exponent and β_l the continuously varying local magnetization exponent. The spatial variation in (6.7) simply follows because $\langle \sigma(y) \rangle$ has the scaling form (6.2) with $\nu = 1$.

The local magnetization exponent varies with the type and strength of the defect according to [108,109]

$$\beta_l = \frac{2}{\pi^2} \arctan^2 \kappa_1 \quad \kappa_1 = e^{-2(K'_1 - K_1)} = \frac{\tanh K'_1}{\tanh K_1} \quad \text{chain defect} \quad (6.8)$$

$$\beta_l = \frac{2}{\pi^2} \arctan^2(\kappa_2^{-1}) \quad \kappa_2 = \frac{\tanh K'_2}{\tanh K_2} \quad \text{ladder defect} \quad (6.9)$$

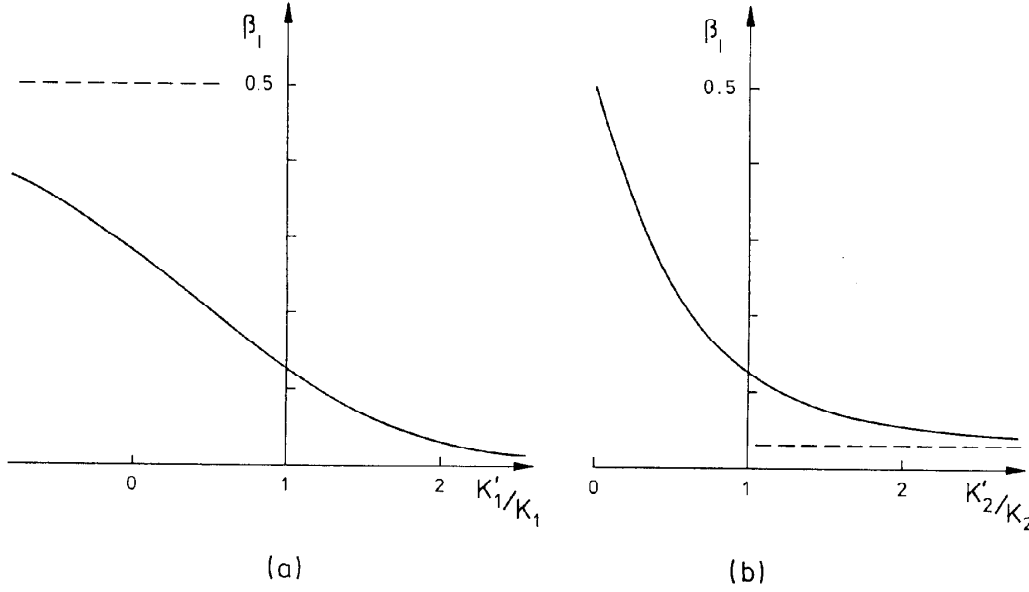


Figure 6.2. Local magnetization exponent β_l vs. defect strength in the Bariev model for (a) chain defect and (b) ladder defect.

where the bulk couplings have their critical values and the asterix denotes dual variables (see below (B2)). These exponents are shown in Figure 6.2.

The chain defect exponent decreases continuously from $\beta_l = 1/2$ when $K'_1 \rightarrow -\infty$ to $\beta_l = 0$ when $K'_1 \rightarrow +\infty$ (Figure 6.2a). In the first limit the spins along the defect are frozen into antiparallel configurations and nearby spins couple to a vanishing total spin. The local exponent then takes the free surface value. In the other limit the vanishing asymptotic value is linked to the onset of local order at the bulk critical point. When $K'_1 = 0$ one can sum out the inner spin and the chain defect effectively becomes a ladder with strength given by $\tanh K'_2 = \tanh^2 K_2$. Then (6.8) and (6.9) give identical results since $\sinh 2K_1 \sinh 2K_2 = 1$ on the critical line.

For a ladder defect the local exponent is invariant under the change $K'_2 \rightarrow -K'_2$ since the original defect coupling can be restored through an appropriate spin reversal in one half of the system. In the positive sector (Figure 6.2b) β_l decreases from the free surface value when $K'_2 = 0$ to a nonvanishing limiting value when $K'_2 \rightarrow +\infty$. Then the ladder is also a chain defect with $K'_1 = 2K_1$ and, with the appropriate values of the perturbed couplings, the two formulae give identical results.

In their study of the spin-spin correlation function parallel to the chain defect McCoy and Perk [109] showed that the correlation length exponent keeps its bulk value $\nu = 1$ although the amplitude of ξ_{\parallel} may depend on the local interaction strength. At the critical point the parallel correlations decay with an exponent $\eta_{\parallel} = 2x_l$ where $x_l = \beta_l$ as expected from scaling, compare (A7).

The incremental specific heat introduced by a chain defect in the square lattice Ising model was obtained by Fisher and Ferdinand [110]. It has a universal exponent $\alpha_l = 1$ corresponding to the expression (A2) with d replaced by d^* .

The energy density correlations were calculated exactly in the scaling region in [111]. Although the correlation function displays much structure, the decay exponents are universal, keeping their bulk values. The same conclusion was reached previously in [112, 113] using the techniques of operator algebra. Although the line defect introduces a marginal operator which is the energy density, this operator has to keep its universal scaling dimension $x = 1$ in order to obtain a continuous variation of β_l with the defect strength: Suppose the dimension of the energy density operator to be changed to $x(\Delta K)$ through the introduction of a defect ΔK . Then a further change of the defect strength would no longer constitute a marginal perturbation since its scaling dimension, given as in (6.5) by $1 - x(\Delta K)$, would be nonvanishing.

Burkhardt and Choi [114] obtained the form of the critical n -point correlation function for the energy density by summing a perturbation series in the defect strength. The complete finite-size behaviour of the transfer matrix spectrum below T_c was investigated in [115].

The Hamiltonian limit of the line defect problem has been studied through real-space renormalization [116] and low-temperature expansion [117]. In this limit one can see a close connection between the line defect problem and the X -ray problem [118] in which correlation functions with continuously varying exponents also occur. Using this analogy [119] one obtains the decay exponents in agreement with (6.8) and (6.9) where, in the Hamiltonian limit (Appendix B.1),

$$\kappa_1 = \frac{K'_1}{K_1^*} \quad \kappa_2 = \frac{K'_2}{K_2} \quad (6.10)$$

The size dependence of the lowest gap in the ordered phase has been investigated through numerical and analytical calculations [120–123].

A one-dimensional quantum hard-dimer model, belonging to the Ising universality class, has also been studied [124]. The novel feature in this case is the jump, with increasing defect strength, from non-universal to ordinary surface behaviour for a critical value of the defect coupling.

Nightingale and Blöte [125] used finite-size scaling on a strip to study line defects in $2d$ models belonging to the Ising universality class as well as in the q -state Potts model. Varying magnetic exponents are obtained in the Ising universality whereas the Potts model

displays bulk behaviour for $q = 1/2$ (irrelevant perturbation) and strong crossover effects for $q = 3$ (relevant perturbation).

The Potts model with a defect line has also been studied through exact renormalization on hierarchical lattices [126]. In the relevant case, with strengthened couplings, the defect remains ordered at the bulk critical point and the system displays a local first order transition [76].

6.3. Conformal invariance, star-like defects

For a system with a line defect the symmetries usually considered to be necessary for conformal invariance (Appendix A.2) are partially broken. This is a similar situation as for a surface. Nevertheless the gap-exponent relations and other spectral properties typical of conformally invariant systems still survive in the marginal Ising case. This was first conjectured on the basis of a numerical study of the classical system mapped onto a strip [127]. The Hamiltonian limit was then studied for larger sizes using fermion techniques [128]. The form of the whole spectrum was conjectured in [129] and exactly calculated in [130].

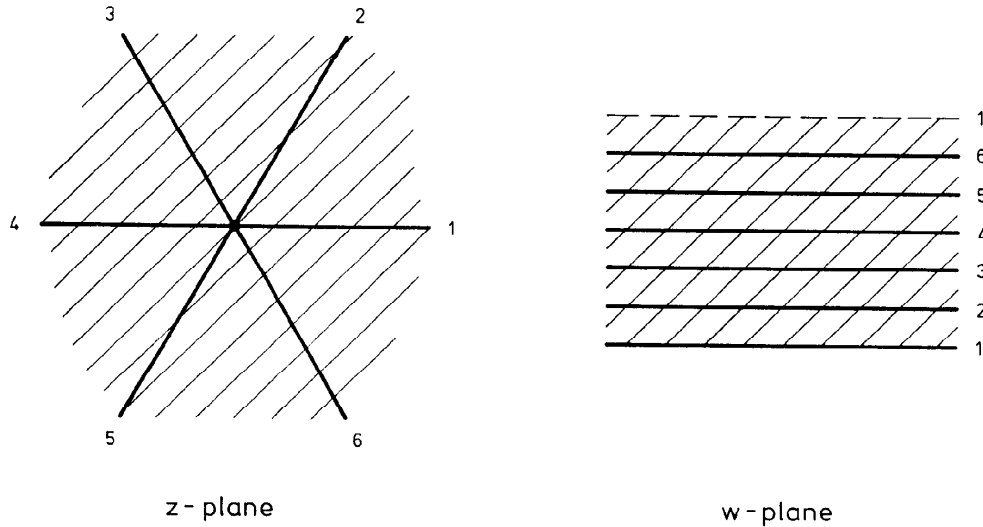


Figure 6.3. A star of defect lines in the z -plane and the corresponding configuration in the periodic strip of the w -plane.

Under the logarithmic mapping (A17) a single infinite defect line in the plane is transformed into a pair of parallel and equidistant lines along a strip with periodic boundary conditions [127]. The same mapping can also be used for star-like defects in the plane [131]. A star with n_d semi-infinite linear branches at the polar angles $\theta_j = 2\pi\delta_j$

($j = 1, \dots, n_d$) is then mapped onto n_d parallel defect lines in a periodic strip of width L (Figure 6.3). With ladder defects, in the extreme anisotropic limit, the Hamiltonian (B3) becomes

$$\mathcal{H} = -\frac{1}{2} \sum_{n=1}^L [\sigma_n^z + \sigma_n^x \sigma_{n+1}^x] + \frac{1}{2} \sum_{j=1}^{n_d} (1 - \kappa_j) \sigma_{L_j}^x \sigma_{L_j+1}^x \quad (6.11)$$

where the defect strength κ_j is the ratio of perturbed to unperturbed couplings like in the second relation (6.10). The defect positions L_j scale with the size of the system as $L\delta_j = L_j - L_{j-1}$.

This Hamiltonian has been diagonalized in [130] using fermion techniques (Appendix B.1). Between the defects the eigenvectors of the excitation matrix have a plane-wave form. The values of the wave-vectors follow from the $2n_d$ boundary conditions at the defects. The conformal properties are preserved only when the δ_j are commensurate. If m is the smallest common denominator of the δ_j 's, either $m = n_d$ for equidistant defects or m is the number of defects in a corresponding equidistant configuration which is obtained by adding $m - n_d$ lines with $\kappa_j = 1$ (Figure 6.3). Then one gets $\gamma(m)$ fermion species in the diagonal Hamiltonian. In the plane this is the number of lines crossing (m even, $\gamma(m) = m/2$) or meeting (m odd, $\gamma(m) = m$) on the star defect in the corresponding equidistant configuration.

The $O(L^{-1})$ part of the Hamiltonian can be written in diagonal form as

$$\mathcal{H}_p = \frac{2\pi\gamma(m)}{L} \sum_{i=1}^{\gamma(m)} \left(\sum_{r=0}^{\infty} \left[\left(r + \frac{1}{2} - \Delta_i\right) \alpha_{ir}^+ \alpha_{ir} + \left(r + \frac{1}{2} + \Delta_i\right) \beta_{ir}^+ \beta_{ir} \right] - \frac{1}{12} \left[\frac{1}{2} - 6\Delta_i^2 \right] \right) \quad (6.12)$$

where α_{ir}^+ (α_{ir}) and β_{ir}^+ (β_{ir}) are fermion creation (annihilation) operators. The shifts Δ_i depend on the κ_j 's and also involve the parity eigenvalues $p = \pm 1$ due to the periodic boundary conditions (see (B6)). When L is even the magnetization and energy sectors of the original Hamiltonian are in correspondence with the odd states of \mathcal{H}_{-1} and the even states of \mathcal{H}_{+1} , respectively. Due to the shifts Δ_i the magnetization sector contains an infinite number of conformal towers.

In the case of a single defect line in the plane the two equidistant lines on the strip have the same strength κ . Then $m = 2$, $\gamma(m) = 1$ and one gets [130]

$$\Delta(\kappa) = 1 - \frac{2}{\pi} \arctan(\kappa^{-1}) \quad p = -1 \quad (6.13)$$

$$\Delta(\kappa) = 0 \quad p = +1 \quad (6.14)$$

The lowest gap gives the dimension of the local magnetization via (A20) and as in (A7)

$$\beta_l = \frac{1}{2} [\Delta(\kappa) - 1]^2 = \frac{2}{\pi^2} \arctan^2(\kappa^{-1}) \quad (6.15)$$

in agreement with the direct calculation in the plane (6.9). When there are several defects, β_l refers to a star and is something like a generalized corner exponent depending on all the defect strengths. In the energy sector the spectrum remains unaffected by the defects and the scaling dimensions are universal. According to (6.12) when $m > 2$ the gap normalization differs by a factor $\gamma(m)$ from the usual one for periodic boundary conditions. This point is discussed in [132]. The spectrum-generating algebra has been obtained in [133] for the single line problem and in [131, 134] for general values of m . Details about this aspect can be found in the review [135].

In addition to the defect problems described so far, the following situations also have been studied. For a 3-state quantum chain with a defect, corresponding to a Potts model, the structure of the spectrum was studied numerically in [136]. A defect where the Pauli matrix σ^x , in one coupling term of the periodic quantum Ising chain, was replaced by a general Hermitian 2×2 matrix was studied in [137]. Exact results could be obtained when the global Z_2 symmetry of the quantum chain is preserved. Then the critical and conformal properties are the same as with an ordinary defect. The same occurs for the Ising quantum chain with staggered 3-spin interactions and the Ashkin-Teller model with generalized defects [138, 139]. Finally, the Ising quantum chain associated with star-like defects was generalized in [140] introducing modified couplings over an extended region. In order to keep the system critical, the same defect strength was taken for the σ^z and σ^x parts in the strip Hamiltonian (B3), which corresponds to a constant change in the anisotropy inside this region. Conformal invariance is preserved, as above for stars, for commensurate configurations. For an arbitrary varying defect amplitude, the equidistant level structure of the spectrum is maintained at high energies only.

7. Extended line defects in the bulk

For defects in the bulk, interesting situations do not only arise if one deals with narrow ones as in Section 6 but also if they are extended as (5.1). This type of problem was first introduced and investigated by Bariev [141–144]. For such extended defects originating from a core of dimension d^* in a d -dimensional system, scaling considerations give two separate relevance-irrelevance criteria. One is associated with the extended part of the defect and is the same as for the surface case. Thus the perturbation is relevant, irrelevant or marginal for $\omega < 1/\nu$, $\omega > 1/\nu$ and $\omega = 1/\nu$, respectively. The other criterion, related to the core of the defect, is the condition on the sign of $d^* - d + 1/\nu$ found below (6.5). The most interesting situation occurs when both conditions predict marginal behaviour. In this case, although the exponents are varying with the defect strength A , there are

discontinuities at $A = 0$ [145]. Connected with that, a perturbation expansion for the exponents is divergent [141]. This feature is outlined in Appendix C.

7.1. Ising model, conformal results

In the two-dimensional Ising model an extended line defect with decay exponent $\omega = 1$ satisfies both marginality conditions since $\nu = 1$. An exact treatment of this problem, however, is more difficult than for the extended surface defect in Section 5, since most of the analytical methods used there cannot be adapted easily to internal defects. The only exception is the method based on conformal mapping.

The problem was treated [145] for a square lattice as in Figure 6.1 with a defect centered at $y = 0$ and couplings $K_2(y)$ varying as

$$K_2(y) = K_2 + \frac{\bar{A}}{|y|} \quad (7.1)$$

where \bar{A} is defined in (5.4) and the bulk couplings K_1, K_2 have the critical values. When $K_2(0) = 0$, the system separates into two uncoupled semi-infinite ones, with a surface inhomogeneity as studied in Section 5.

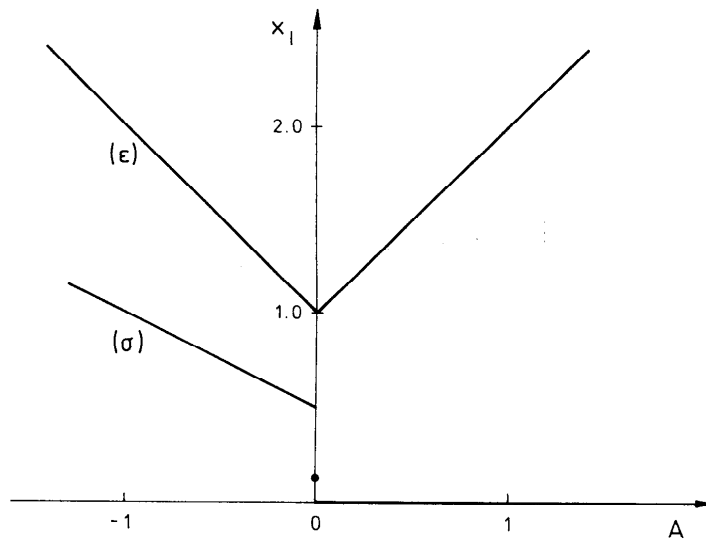


Figure 7.1. Local scaling dimensions for spin (σ) and energy density (ε) for an extended defect with $\omega=1$ in the bulk of an Ising model as a function of the strength A .

Using the logarithmic transformation (A17) the problem is mapped onto a strip. The inhomogeneity thereby becomes periodic with period $L/2$ and is given by

$$\Delta K(u) = \overline{A} \left| \frac{L}{2\pi} \sin \left(\frac{2\pi u}{L} \right) \right|^{-1} \quad (7.2)$$

In each of the intervals, up to a factor of two, this has the same form as (5.13).

As in Section 5.3 the lowest gaps were determined in a continuum approximation. Due to the different boundary conditions, the eigenvalues and hence, the local critical exponents are different from those in the surface defect problem. The scaling dimensions are shown in Figure 7.1 as functions of A .

For enhanced local couplings ($A > 0$) the energy of the lowest excited state, $E_1 - E_0 \sim L^{-1-2A}$, vanishes faster than $1/L$ so that the scaling dimension of the magnetization is $x_l = 0$ and the defect region remains ordered at the bulk critical point. On the other hand for reduced couplings ($A < 0$) there is no order at $T = T_c$ and the local exponents are linear functions of A . The magnetic exponent is the same as for two disconnected semi-infinite systems (see Figure 5.2). At $A = 0$ it is discontinuous. As a consequence a finite-order perturbation expansion for the gaps around the homogeneity point $A = 0$ is not possible. The expansion for the first gap starts as [145]

$$E_1 - E_0 = \frac{2\pi}{L} \left(\frac{1}{8} - \frac{A}{\pi} \log L + \dots \right) \quad (7.3)$$

i.e. the first-order correction term is divergent, but the singular contributions sum up to a regular term in infinite order. This observation is in agreement with the results of the perturbation theory for the system in the original geometry (Appendix C).

The critical exponent for the energy operator given by

$$x_l = 1 + |A| \quad (7.4)$$

is continuous at $A = 0$ where it reaches its bulk value. It can be determined independently, working in the plane and using finite-size scaling for the matrix-element of the local energy operator as in (A21). The coincidence of the two results supports the assumption that the system is conformally invariant at the critical point.

8. Radially extended defects

The systems studied so far had essentially all a layered structure. As a final example, we now examine the case where the inhomogeneity extends radially. The centre may be located either in the bulk or on a free surface. Only marginal temperature-like perturbations corresponding to a change in the interaction strength are considered. After some scaling considerations, exact results for the local magnetization in the two-dimensional Ising model are presented. This is supplemented by a discussion of the conformal aspects.

8.1. Scaling considerations

According to the scaling arguments of Section 6.1, a short-range perturbation introduced by a point defect with $d^* = 0$ into a d -dimensional system has a scaling dimension $-d + 1/\nu$ which follows from (6.5). Since $1/\nu < d$ at a second order phase transition this type of perturbation is always irrelevant. This can be verified explicitly for the Ising model through a calculation of the local magnetization which may be expressed in terms of averages for the unperturbed system [146]. Following the method of Section 2.2 and using the rotational symmetry one can also obtain the critical correlation functions. They are completely determined and identical to the unperturbed ones.

In the case of an extended defect and a perturbation amplitude decaying as a power of the distance from the centre, the relevance-irrelevance criterion is the same as for perturbations decaying from an interior line defect or a surface (Sections 5, 7 and Appendix C). For a temperature-like perturbation, according to Equations (5.2) and (C7), the amplitude has a scaling dimension $1/\nu - \omega$ where ω is the decay exponent of the perturbation. In the following we consider the marginal case where $\omega = 1/\nu$.

8.2. Ising model

For the Ising model containing an extended defect with $\omega = 1$ exact results were obtained using the corner transfer matrix method [147].

The section of a square lattice forming the corner transfer matrix is shown in Figure B1b. For the present problem one chooses anisotropic couplings K_1 and

$$K_2(n) = K_2 \left(1 + \frac{\alpha}{2n+1} \right) \quad (8.1)$$

where n is the row index increasing from the centre. The Hamiltonian limit leads to a study of an inhomogeneous quantum chain (B3) with couplings $h_n = 2n$, $\lambda_n = \lambda(2n + \alpha + 1)$. As it stands, the corner transfer matrix describes a segment of an anisotropic system with

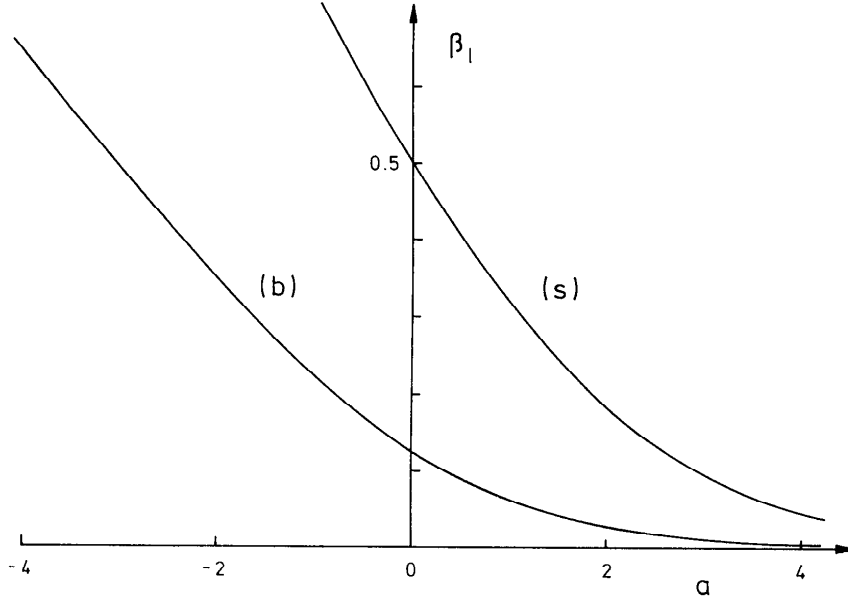


Figure 8.1. Local magnetization exponent β_l vs. defect strength for a radially extended defect (b) in the bulk and (s) on the surface of an isotropic Ising model. Here a is equal to $\pi\alpha$.

opening angle 90° . However, as explained in Appendix B.3, it also describes an isotropic system for which the opening angle is infinitesimal. Therefore an isotropic system with rotational symmetry and opening angle θ can be described by the transfer matrix

$$\mathcal{T}(\theta) = \exp\left(-\frac{1}{2}\theta\mathcal{H}\right) \quad (8.2)$$

According to (B19) the magnetization at the centre involves the single particle excitations ω_l of the quantum chain. The critical excitation spectrum can be obtained by taking the continuum limit. Then the very centre of the system has to be excluded [148]. Taking a cut-off at r and an outer radius R , the critical excitations are given by

$$\omega_l = \sqrt{\alpha^2 + \left(\frac{2z_l}{\ln R/r}\right)^2} \quad (8.3)$$

where the z_l are solutions of $\alpha \ln(R/r) \tan z = -2z$. An additional bound-state-like solution occurs when $\alpha < 0$. The local magnetization exponent β_l then follows from the finite-size behaviour of the centre magnetization which is analogous to (A8). This gives

$$\beta_l = \frac{\alpha^2}{2} \int_0^\infty du \frac{\sinh^2 u}{\sinh(\pi |\alpha| \cosh u)} \quad (8.4)$$

A bound-state contribution $|\alpha|/2$ must be added when $\alpha < 0$. The variation of the magnetization exponent with the perturbation strength is shown in Figure 8.1. The

exponent decreases smoothly when the defect amplitude is increased but, contrary to the case of surface or extended line defects, it vanishes only asymptotically. Thus there is no local order at the bulk critical point for any finite value of the defect strength.

8.3. Conformal considerations

The previous Ising results can also be deduced from a mapping of the perturbed critical system onto a strip [149, 150]. This mapping can be done for an arbitrary conformally invariant two-dimensional system containing an extended perturbation with rotational symmetry. Then, in the continuum limit,

$$-\beta\mathcal{H} = -\beta\mathcal{H}_c + g \int r^{-\omega} \psi(r, \theta) r dr d\theta \quad (8.5)$$

where $\psi(r, \theta)$ is some local field with scaling dimension x_ψ . In the following, as before, we assume that the decay exponent takes its marginal value $\omega = 2 - x_\psi$. Under the transformation (A17) the dilatation factor just compensates the decay of the perturbation in the marginal case. Therefore, in the periodic strip of width L , one obtains an homogeneous L -dependent deviation from criticality

$$\Delta = g \left(\frac{2\pi}{L} \right)^{2-x_\psi} \quad (8.6)$$

for the couplings which are conjugate to ψ . One should note that such a homogeneous deviation from the bulk critical couplings leads to a massive excitation spectrum as in (8.3) and, contrary to the case of extended line defects treated in Sections 5 and 7, the tower-like, equidistant-level structure of the spectrum is lost here.

Let ϕ , with bulk scaling dimension x , be either the energy or the magnetization density. Its local scaling dimension at the defect, x_l , can be deduced from the corresponding gaps for the strip through (A20). According to finite-size scaling, the perturbed gap G_ϕ transforms as

$$G_\phi(\Delta, L) = L^{-1} G_\phi(L^{2-x_\psi} \Delta, 1) = L^{-1} f_\phi [(2\pi)^{2-x_\psi} g] \quad (8.7)$$

where f_ϕ is a universal scaling function [151]. This leads to the local exponent

$$x_l = \frac{1}{2\pi} f_\phi [(2\pi)^{2-x_\psi} g] \quad (8.8)$$

It depends on the perturbation amplitude g , as expected for a marginal perturbation, but does it in an universal way [150]. Different systems belonging to the same class of universality will show the same dependence on the perturbation amplitude.

For the Ising model, the perturbed gaps (or gap scaling functions) can be calculated either for an isotropic strip or using the Hamiltonian limit [152–155]. In the latter case the defect amplitude has to be rescaled as discussed in Appendix B.3. On a square lattice with modified interactions $K(r) = K_c + A/r$ one recovers the local magnetic exponent given in (8.4) with $\alpha = 8A$ [149]. For small values of A , it has the expansion

$$\beta_l = x_l = \frac{1}{8} - 2A + 16 \ln 2 A^2 + O(A^3) \quad (8.9)$$

To first order this is identical to the perturbation result in Table C2 with $g = 2A$. The factor of two in the continuum parameter g reflects the two bonds per unit cell on the square lattice. Due to the dual symmetry of the Ising model [156] the exponent of the local energy density has an expansion involving only even powers of the perturbation amplitude and reads [150]

$$x_l = 1 + 32A^2 + O(A^4) \quad (8.10)$$

The same procedure applies with minor changes when the defect centre is located on a free surface. This was also studied for the Ising model [149]. To first order the result is again in agreement with the perturbation approach (Table C2). The corresponding magnetic exponent is also shown in Figure 8.1.

9. Conclusion

In this review we have presented a number of systems and situations where the universality which is normally found at continuous phase transitions can be absent. Superficially, the examples look quite different, but in each case the tendency towards order is modified locally in a particular systematic way. This is the basis for the common features one observes.

It is not difficult to understand the results qualitatively. For example, if order is favoured this leads to a steeper magnetization curve and will tend to reduce the magnetic exponent. This explains the general form and the similarity of the graphs in the various marginal cases. There are, of course, some differences in details. The close parallel between effects from the geometry and from the modification of interactions inside a system is nevertheless remarkable. A similar relation is found if one compares homogeneous integrable systems at and off the critical point [35, 157, 158, 48]. In this case the corner transfer matrix can be used as a link. For the present systems the direct connection is less obvious.

In two dimensions conformal mappings play an important rôle in the studies. The results show that they can be used even beyond their obvious domain. The gap-exponent

relation also holds in cases like in Section 8 where no tower of equidistant levels exists. This is an aspect which might deserve further study. The same is true for the situation in three dimensions where only a few, essentially mean field results have been obtained so far.

The last point is also important since it should be possible to measure some of the effects. The most obvious experiment would be to look for the local order in systems with wedge-like, conical or parabolic shape. This is not easy since the local order will be smaller than inside the bulk, and already for planar surfaces such measurements are rare. Nevertheless they should be feasible with proper local probes and would add an interesting aspect to the general picture of critical phenomena.

Acknowledgments

This work is the result of a collaboration with mutual visits of the authors to Nancy, Berlin and Budapest. F. I. is indebted to the Ministère Français des Affaires Etrangères and the CNRS for research grants. I. P. thanks the University of Nancy I and the Research Institute for Solid State Physics in Budapest for hospitality. L. T. acknowledges the support of DFG, Projekt "Zweidimensionale kritische Systeme" and together with F. I. the support of the CNRS and the Hungarian Academy of Sciences through an exchange project. The authors benefitted from conversations with R. Z. Bariev and B. Berche.

Appendix A. Scaling and conformal invariance

Near a second order phase transition the singular parts of thermodynamic quantities vary as powers of the parameters (scaling fields) $t \sim |T - T_c|$, h , etc. measuring the deviation from the critical point. This type of behaviour is linked to the self-similarity of critical fluctuations inside the correlation volume ξ^d where $\xi \sim t^{-\nu}$ is the correlation length. The system is then covariant under a global change of the length scale and singular quantities are homogeneous functions of their arguments. These properties form the basis of the scaling hypothesis [159] which lead to scaling laws relating critical exponents to a small number of fundamental ones. The scaling behaviour was also the source of the renormalization group ideas [1], allowing a calculation of the fundamental exponents.

At the critical point, ξ diverges and the system becomes scale invariant. This, together with more usual symmetries (rotation, translation), leads to the invariance under conformal transformation, first used in field theory [160] and later fully exploited in two-dimensional critical systems where it allows an exact determination of the critical exponents and much more [161, 16, 162].

A.1. Scaling and critical exponents

According to scaling theory, when the lengths are rescaled by a factor $b > 1$, i.e. when $\mathbf{r} \rightarrow \mathbf{r}/b$, the scaling fields (like t and h) are changed by a factor b^{d-x} where d is the dimension of the system and x the scaling dimension of conjugate quantities (e.g. the energy density for t , the magnetization density for h). When $d - x > 0$ (< 0) the corresponding scaling field grows (decreases) under rescaling. Such a field is said to be relevant (irrelevant) whereas it is marginal when $x = d$. The system becomes invariant under rescaling only when the relevant scaling fields vanish which corresponds to the critical point.

Since irrelevant variables finally vanish under rescaling, only relevant and marginal scaling fields influence the critical properties, the marginal ones generally leading to varying exponents.

Near the critical point, the singular part of the free energy density is a homogeneous function of the scaling fields and transforms according to

$$f_b \left(t, h, \frac{1}{L} \right) = b^{-d} f_b \left(b^{1/\nu} t, b^{d-x} h, \frac{b}{L} \right). \quad (\text{A1})$$

In (A1) we kept only relevant variables and included the inverse of the linear size of the system as a new relevant scaling field, since at its bulk critical point a system is truly critical only in the thermodynamic limit, i.e. when $1/L = 0$.

The critical behaviour of conjuguate quantities and their derivatives can be deduced from (A1) taking advantage of the arbitrariness of the dilatation factor b . The corresponding exponents are all related to the basic ones x , ν through scaling laws and involve d .

For example, the specific heat exponent α can be obtained from the second t -derivative of both sides of (A1) at $h = 0$, $1/L = 0$ and taking $b = t^{-\nu}$ with the result

$$\alpha = 2 - d\nu \quad (\text{A2})$$

The magnetization $m = -\partial f_b / \partial h$ transforms as

$$m\left(t, h, \frac{1}{L}\right) = b^{-x} m\left(b^{1/\nu} t, b^{d-x} h, \frac{b}{L}\right) \quad (\text{A3})$$

and the exponent β , defined through $m \sim t^\beta$, can be obtained from (A3) taking $h = 0$, $1/L = 0$ and $b = t^{-\nu}$ as before, so that

$$\beta = \nu x. \quad (\text{A4})$$

At the bulk critical point $t = 0$, $h = 0$, critical singularities are suppressed by a finite L value. Finite-size scaling exploits the way they develop when $L \rightarrow \infty$ in order to determine the critical exponents. For example, from (A1) with $b = L$, the free energy density behaves as L^{-d} at criticality whereas the magnetization density in (A3) gives

$$m(L) \sim L^{-x}. \quad (\text{A5})$$

When the system is limited in space through a surface, besides the bulk term f_b in (A1), new local contributions (surface, corner, etc.) to the free energy density appear, with singular parts behaving as above for the bulk. For example, the contribution of a surface with dimension $d - 1$ transforms according to [4]

$$f_s\left(t, h_s, \frac{1}{L}\right) = b^{-(d-1)} f_s\left(b^{1/\nu} t, b^{d-1-x_s} h_s, \frac{b}{L}\right). \quad (\text{A6})$$

where a surface magnetic field h_s has been included. Repeating the previous argument, the scaling relations (A4–5) remain valid with the appropriate surface exponents replacing bulk ones,

$$\beta_s = \nu x_s, \quad (\text{A7})$$

$$m_s(L) \sim L^{-x_s}. \quad (\text{A8})$$

The surface susceptibility exponent γ_s defined through $\partial^2 f_s / \partial h_s^2 \sim t^{-\gamma_s}$ is obtained as

$$\gamma_s = \nu(d - 1 - 2x_s). \quad (\text{A9})$$

The bulk two-point correlation function for an operator ψ is obtained taking a functional derivative of the free-energy with respect to the appropriate position-dependent field

$$G(r, t) \equiv \langle \psi(0)\psi(\mathbf{r}) \rangle = \frac{\delta^2 F}{\delta h(0)\delta h(\mathbf{r})}. \quad (\text{A10})$$

If e.g. $\psi(\mathbf{r})$ stands for the magnetization operator, then its average $\langle \psi(\mathbf{r}) \rangle = m(\mathbf{r})$ gives the local magnetization. The transformation law of the two-point function then follows from (A10) and (A1)

$$G(r, t) = b^{-2x} G\left(\frac{r}{b}, b^{1/\nu} t\right) \quad (\text{A11})$$

where x is the bulk scaling dimension of ψ . At the critical point, $t = 0$, taking $b = r$, the power-law decay of correlations follows

$$G(r, t = 0) = \frac{A}{r^{2x}}. \quad (\text{A12})$$

Surface correlations can be investigated in the same way. The correlation function with two points at the surface behaves as

$$G_{\parallel}(r, t = 0) \sim r^{-2x_s} \quad (\text{A13})$$

while the perpendicular correlations decay like $r^{-(x+x_s)}$ (see Section 2.2).

A.2. Conformal invariance

Covariance under conformal transformations is expected to hold at the critical point of systems with short range interactions, which possess translational and rotational symmetry and are invariant under uniform scaling. When some of the above symmetries are broken by a marginal perturbation (e.g. for inhomogeneous systems) some of the properties associated with conformally invariant systems, like the gap-exponent relation, can be preserved as observed in specific examples.

A conformal transformation $\mathbf{r} \rightarrow \mathbf{r}'(\mathbf{r})$ can be seen as a generalization of uniform scaling, where the structure of the lattice is locally preserved, but the rescaling factor $b(\mathbf{r})$ becomes a smooth function of the position. It follows from the Jacobian of the

transformation as $b(\mathbf{r})^{-d} = \det(\partial \mathbf{r}' / \partial \mathbf{r})$. Since local fields transform as $h(\mathbf{r}) \rightarrow h'(\mathbf{r}') = b(\mathbf{r})^{d-x} h(\mathbf{r})$ the two-point function in (A10) transforms like

$$\langle \psi(\mathbf{r}_1) \psi(\mathbf{r}_2) \rangle = b(\mathbf{r}_1)^{-x} b(\mathbf{r}_2)^{-x} \langle \psi(\mathbf{r}'_1) \psi(\mathbf{r}'_2) \rangle \quad (\text{A14})$$

under a conformal transformation. This is a straightforward generalization of (A11) with $t = 0$. Similarly the transformation law for an operator profile $\langle \psi(\mathbf{r}) \rangle$ is obtained as

$$\langle \psi(\mathbf{r}) \rangle = b(\mathbf{r})^{-x} \langle \psi(\mathbf{r}') \rangle. \quad (\text{A15})$$

The conformal group for dimensions larger than two is finite-dimensional and contains rotations, uniform dilatations, translations and inversions. The special conformal transformation with an arbitrary translation \mathbf{a} ,

$$\frac{\mathbf{r}'}{r'^2} = \frac{\mathbf{r}}{r^2} + \mathbf{a}, \quad (\text{A16})$$

is constructed from the two last ones. Invariance under this transformation fixes the form of three-point functions [160] like scaling does with the two-point functions in (A12) and (A13). If \mathbf{a} in (A16) is an infinitesimal surface vector, then one can use this transformation to find restrictions on the form of surface correlations, as shown in Section 2.2.

The method of conformal invariance is especially powerful in two dimensions where the conformal group, being isomorphic with the group of complex analytic functions, becomes infinite-dimensional and strongly restricts the possible values of critical exponents for a broad class of systems [161, 163, 16, 162].

In two dimensions one may also use a complex mapping $w(z)$ to go from one geometry to another [164]. When some critical correlation is known in the first geometry, it can be transformed into the second one. The local dilatation factor is then $b(z) = |dw/dz|^{-1}$.

Two basic geometries are connected by the logarithmic transformation

$$w = \frac{L}{2\pi} \ln z \quad (\text{A17})$$

which maps the infinite z -plane onto a periodic strip of width L in the w -plane. Transforming the correlation function in (A12) according to (A14), one obtains

$$\langle \psi(u_1, v_1) \psi(u_2, v_2) \rangle = \frac{(2\pi/L)^{2x}}{\left[2 \cosh \frac{2\pi}{L}(u_1 - u_2) - 2 \cos \frac{2\pi}{L}(v_1 - v_2) \right]^x} \quad (\text{A18})$$

in the strip geometry where u measures the distance along the strip and $0 < v \leq L$ denotes the transverse periodic coordinate. An expansion of the r.h.s. of (A18) for $u_1 > u_2$ leads to

$$\begin{aligned} \langle \psi(u_1, v_1) \psi(u_2, v_2) \rangle = & \left(\frac{2\pi}{L} \right)^{2x} \sum_{m, \bar{m}}^{\infty} a_m a_{\bar{m}} \exp \left[-\frac{2\pi}{L} (x + m + \bar{m})(u_1 - u_2) \right] \\ & \times \exp \left[\frac{2i\pi}{L} (m - \bar{m})(v_1 - v_2) \right] \end{aligned} \quad (\text{A19})$$

where $a_m = \Gamma(x + m)/\Gamma(x)m!$. The strip correlation function can be also determined through a direct calculation using the transfer matrix method as described in Appendix B. Then, comparing (A19) with expressions like (B13), one reaches the following conclusions:

i) The eigenstates of the Hamiltonian in (B1) are labelled by pairs of integers (m, \bar{m}) , so that the spectrum exhibits a tower-like structure with energies $E_0 + (x + m + \bar{m}) 2\pi/L$ and momenta given by $(m - \bar{m}) 2\pi/L$.

ii) The gap between the ground state and the lowest excited state for which the matrix element of ψ is non-vanishing, is related to the scaling dimension x via

$$E_1 - E_0 = \frac{2\pi}{L} x. \quad (\text{A20})$$

This is the gap-exponent relation.

iii) Finally, the matrix element itself is given as

$$\langle 1 | \psi | 0 \rangle = \left(\frac{2\pi}{L} \right)^x \quad (\text{A21})$$

For the magnetization, this is in agreement with the finite-size scaling result (A5).

To study surface correlations, the half-plane ($y > 0$) can be mapped onto a strip with free boundaries through the conformal transformation

$$w = \frac{L}{\pi} \ln z. \quad (\text{A22})$$

Now the eigenstates of the Hamiltonian in the strip are labelled by an integer $m = 0, 1, \dots$, the spectrum has a tower-like structure with energy eigenvalues $E_0 + (x_s + m)\pi/L$ and the gap-exponent relation reads

$$E_1 - E_0 = \frac{\pi}{L} x_s. \quad (\text{A23})$$

Finally, the matrix element for ψ near the boundary is given by

$$\langle 1 | \psi_s | 0 \rangle = \left(\frac{\pi}{L} \right)^{x_s}. \quad (\text{A24})$$

Appendix B. Transfer Matrices

In the transfer matrix method [156, 165, 166] a system of spins or other classical variables with short-range interactions is built from identical smaller units. This technique can also be used for the inhomogeneous systems considered here. In two dimensions one can choose the basic units as shown in Figure B1. The corresponding transfer matrices \mathcal{T} are the partition functions of either two consecutive rows (case a) or a whole angular segment (case b). Their matrix character results from their dependence on the two sets $\{\sigma\}, \{\sigma'\}$ of boundary spins (full points). The partition function Z of the whole system is then obtained by taking the product of an appropriate number of \mathcal{T} 's. For periodic boundary conditions in the direction of transfer, Z is given by the trace over this product and for free boundary conditions by a particular matrix element. Thermal expectation values can be calculated by inserting additional operators. In this way, the complete thermodynamical behaviour is contained in \mathcal{T} .

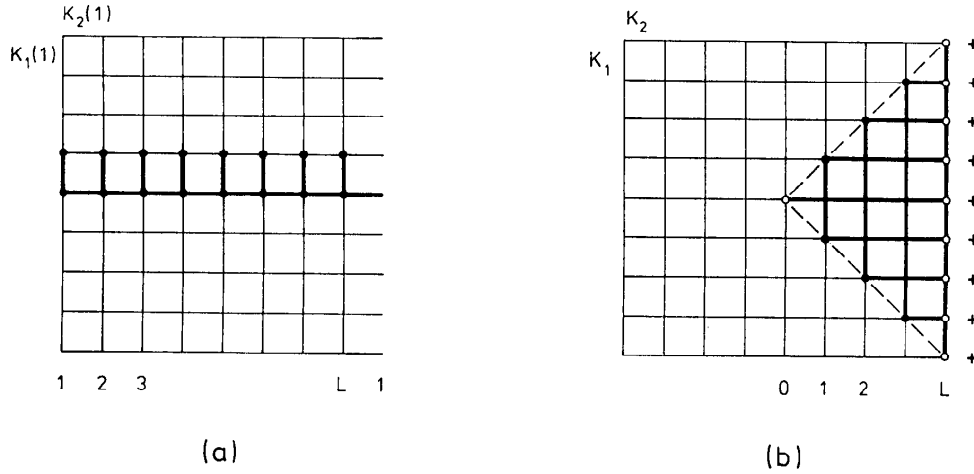


Figure B1. Sections of a square lattice (thick) which form (a) the row transfer matrix and (b) the corner transfer matrix. Open circles correspond to fixed spins.

It is customary to write the transfer matrices as

$$\mathcal{T} = \exp(-H) \quad (B1)$$

in analogy with time evolution operators. For the Ising model, \mathcal{T} can be expressed in terms of Pauli matrices and the corresponding H may be regarded as the Hamiltonian for a certain spin one-half quantum chain. In the following this is described in some detail.

B.1. Row transfer matrix

This quantity (Figure B1a) is appropriate for a homogeneous system or a layered one with couplings $K_i(n)$ varying along the horizontal direction. It is given explicitly by [167]

$$\mathcal{T} = \exp \left[\sum_n K_1^*(n) \sigma_n^z \right] \exp \left[\sum_n K_2(n) \sigma_n^x \sigma_{n+1}^x \right] \quad (B2)$$

where the $K_1^*(n)$ are dual couplings ($\tanh K_1^* = \exp(-2K_1)$) and periodic boundary conditions are assumed horizontally, $\sigma_{L+1}^\alpha = \sigma_1^\alpha$. An open system can be obtained by setting one $K_2(n)$ equal to zero.

The matrix \mathcal{T} , or its symmetrized versions one uses normally, can in principle be diagonalized for arbitrary couplings [168, 78]. In this sense, the two-dimensional Ising model is called a completely integrable system. A considerable simplification occurs, however, in the anisotropic (Hamiltonian) limit of strong vertical and weak horizontal bonds [169, 170, 135]. Then $K_1^*(n)$ and $K_2(n)$ are both small and one can combine the exponentials to obtain $H = 2K_1^* \mathcal{H}$, where K_1^* is some reference value and

$$\mathcal{H} = -\frac{1}{2} \sum_{n=1}^L h_n \sigma_n^z - \frac{1}{2} \sum_{n=1}^L \lambda_n \sigma_n^x \sigma_{n+1}^x \quad (B3)$$

This is the Hamiltonian of an Ising chain with couplings λ_n and transverse fields h_n . The normalization is such that for $h_n = \lambda_n = 1$ the excitations have velocity one.

The operator \mathcal{H} can be expressed in terms of Fermi operators c_n, c_n^+ via the Jordan-Wigner transformation [171, 167, 172]

$$\sigma_n^+ = c_n^+ \exp \left(i\pi \sum_{l=1}^{n-1} c_l^+ c_l \right) \quad (B4)$$

$$\sigma_n^z = 2c_n^+ c_n - 1 \quad (B5)$$

This gives

$$\mathcal{H} = -\sum_{n=1}^L h_n \left(c_n^+ c_n - \frac{1}{2} \right) - \frac{1}{2} \sum_{n=1}^{L-1} \lambda_n (c_n^+ - c_n)(c_{n+1}^+ + c_{n+1}) + \frac{1}{2} \lambda_L (c_L^+ - c_L)(c_1^+ + c_1) \mathcal{P} \quad (B6)$$

where $\mathcal{P} = (-1)^L \prod_n \sigma_n^z = \exp(i\pi \sum_n c_n^+ c_n)$. This operator with eigenvalues $p = \pm 1$ commutes with \mathcal{H} and distinguishes subspaces with even and odd fermion number. In each subspace \mathcal{H} is diagonalized by a Bogoljubov transformation [80, 173]. In terms of new operators α_q, α_q^+ it takes the form

$$\mathcal{H} = \sum_q \varepsilon_q \left(\alpha_q^+ \alpha_q - \frac{1}{2} \right) \quad (B7)$$

The single-fermion eigenvalues ε_q follow from a $L \times L$ matrix equation which reads, in the notation of reference [80]

$$(\mathbf{A} - \mathbf{B})(\mathbf{A} + \mathbf{B})\Phi_q = \varepsilon_q^2 \Phi_q \quad (B8)$$

with the matrix given by

$$\begin{pmatrix} h_1^2 + \lambda_L^2 & h_1 \lambda_1 & & & -p h_L \lambda_L \\ h_1 \lambda_1 & h_2^2 + \lambda_1^2 & h_2 \lambda_2 & & \\ & \ddots & \ddots & \ddots & \\ & & h_{L-2} \lambda_{L-2} & h_{L-1}^2 + \lambda_{L-2}^2 & h_{L-1} \lambda_{L-1} \\ -p h_L \lambda_L & & & h_{L-1} \lambda_{L-1} & h_L^2 + \lambda_{L-1}^2 \end{pmatrix} \quad (B9)$$

For a homogeneous system the equations are solved by Fourier transformation. The fermion states are running waves with momenta q given by $q = 2n\pi/L$ ($p = -1$) or $q = (2n+1)\pi/L$ ($p = +1$) and integers n such that $|q| \leq \pi$. Putting $h_n = 1$, $\lambda_n = \lambda$, the eigenvalues are

$$\varepsilon_q = (1 + \lambda^2 - 2\lambda \cos q)^{1/2}. \quad (B10)$$

This expression is the Hamiltonian limit of Onsager's general result [174]

$$\cosh \omega_q = \cosh 2K_1^* \cosh 2K_2 - \sinh 2K_1^* \sinh 2K_2 \cos q \quad (B11)$$

where $\omega_q = 2K_1^* \varepsilon_q$.

If one multiplies a large number of \mathcal{T} 's, their largest eigenvalues are most important. They are given by the smallest ones of \mathcal{H} . The two lowest states of \mathcal{H} are the ground states in the two subspaces $p = \pm 1$. If $\lambda > 1$, they become degenerate for $L \rightarrow \infty$ and this leads to the appearance of long-range order in the system.

If the system has free ends, no distinction occurs between $p = \pm 1$. The solutions are standing waves with q -values determined by the boundary conditions. For $\lambda > 1$ one finds an additional solution with imaginary wave number, localized near one surface. The corresponding eigenvalue vanishes exponentially as $L \rightarrow \infty$ so that this state is again related to the long-range order. In particular, it determines the surface magnetization (cf. Section 5.2).

At the critical (self-dual) point $h = \lambda = 1$ the eigenvalues are

$$\varepsilon_q = 2 \left| \sin \frac{q}{2} \right|. \quad (B12)$$

The q -values for the homogeneous case are given above, while for free ends $q = (2n+1)\pi/(2L+1)$ and $0 \leq q < \pi$. The low-lying part of the spectrum has a linear energy-momentum relation, $\varepsilon_q = q$, and the towers of equidistant eigenvalues are in complete

agreement with the conformal predictions (Appendix A). The left- and right-moving particles in the homogeneous system correspond to the two Virasoro algebras present in this case.

The layered systems treated in Sections 5-7 are special cases of the problem formulated in (B3) or (B8-9).

For periodic boundary conditions the existence of two subspaces leads to considerable complications if an operator like σ^x connects the two. Thus a spin correlation function in the direction of the transfer has the form

$$\langle \sigma_l^x \sigma_0^x \rangle = \sum_m |\langle m, -p | \sigma^x | 0, p \rangle|^2 \exp[-l(E_m(-p) - E_0(p))] \quad (B13)$$

The non-universal behaviour of this function for the case of a line defect (Section 6) can be related to its particular structure involving both subspaces [119].

B.2. Corner transfer matrix

This quantity is the partition function for a whole angular segment of a lattice. For the case shown in Figure B1b it is a 90° segment. The inner variables are supposed to be summed over. The partition function of the total system is then given by the trace over the product of four such 90° matrices. If the system is invariant under 90° rotations, all matrices are identical. Otherwise one has two different types. The importance of these matrices is connected with their use in calculating order parameters. For this the variables along the outer boundary are fixed as shown and the order at site 0 is considered in the thermodynamic limit. That this is a practical and quite efficient procedure was noted by Baxter who introduced this type of transfer matrix and studied it for various solvable models [175, 176, 6, 177].

From Baxter's results it follows that the operator \mathcal{H} related to the corner transfer matrix of a homogeneous Ising model has again the form (B3). In the Hamiltonian limit this can be seen directly. The coefficients h_n , λ_n then follow from the geometry and are proportional to the number of vertical and horizontal bonds at distance n from the tip, respectively

$$h_n = 2n \quad \lambda_n = \lambda(2n + 1) \quad n = 0, 1, \dots, (L - 1) \quad (B14)$$

In addition $h_L = 0$ due to the fixed boundary spins. The resulting eigenvalue problem (B8-9) can be solved via generating functions and special polynomials [178, 179]. Due to

the boundary conditions, one eigenvalue is zero. The other low-lying eigenvalues in the ordered phase ($\lambda > 1$) are, with q replaced by l

$$\varepsilon_l = (2l - 1)\varepsilon \quad l = 1, 2, \dots \quad (B15)$$

where $\varepsilon = \pi\lambda/2\mathbf{K}(1/\lambda)$ and \mathbf{K} is the complete elliptic integral of the first kind. This result also follows by taking the Hamiltonian limit in the general formula for the eigenvalues $\omega_l = 2K_1^*\varepsilon_l$ of the infinite system [6]

$$\omega_l = (2l - 1) \frac{\pi u}{2\mathbf{K}(k)} \quad (B16)$$

where $k = (\sinh 2K_1 \sinh 2K_2)^{-1}$ and u , measuring the anisotropy, is defined via the elliptic function sn by $\sinh 2K_2 = -i \text{sn}(iu, k)$. The equidistance of the levels ε_l, ω_l which directly reflects the geometry, is a very remarkable property. Such a level structure is also found for the corner transfer matrices of other integrable models. From (B16) it follows that near criticality the ω_l scale as $1/\ln(1/t)$. Thus the spectrum collapses at the critical point, but (B15) still holds for a large finite system. Then $\varepsilon \cong \pi/\ln L$ in agreement with conformal predictions [35, 180, 181].

For radially inhomogeneous systems as in Section 8.2, the coefficients h_n, λ_n are modified compared to (B14). The same holds if the shape is different from a wedge, as in Section 4.3.

The magnetization $\langle \sigma_0 \rangle$ in the centre of a system built from m segments and closed upon itself, can be written as

$$\langle \sigma_0 \rangle = \frac{Z_+ - Z_-}{Z_+ + Z_-} \quad (B17)$$

where Z_+ and Z_- are the partition functions with σ_0 parallel and antiparallel to the boundary spins, respectively. In terms of the corner transfer matrix \mathcal{T} of one segment this becomes a quotient of traces

$$\langle \sigma_0 \rangle = \frac{\text{Tr}(\sigma_0^x \sigma_N^x \mathcal{T}^m)}{\text{Tr}(\mathcal{T}^m)} \quad (B18)$$

The operator $\sigma_0^x \sigma_N^x$ measures the relative orientation of the spin at 0 and the outer spins. It can be expressed in terms of the Fermi operators which diagonalize \mathcal{T} as $\exp(i\pi \sum_l \alpha_l^+ \alpha_l)$ where $l \geq 1$. Thus it distinguishes states with even or odd number of excited fermions. Inserting (B1) and the diagonal form of H , the traces can be performed independently over the single-fermion states and one obtains the magnetization in the form of a product

$$\langle \sigma_0 \rangle = \prod_l \tanh\left(\frac{m\omega_l}{2}\right) \quad (B19)$$

This is a central result of the corner transfer matrix approach.

One may note that the formula (B19) is identical to the one for the corresponding end magnetization of an inhomogeneous Ising chain with couplings $m\omega_l/2$. Onsager's result [182] for the spontaneous bulk magnetization $\langle \sigma_0 \rangle = (1 - k^2)^{1/8}$ follows directly from it by setting $m = 4$ and using (B16) together with elliptic function identities. As mentioned in Section 3.2, the situation is more complicated for systems having free edges [34].

B.3. Rescaling

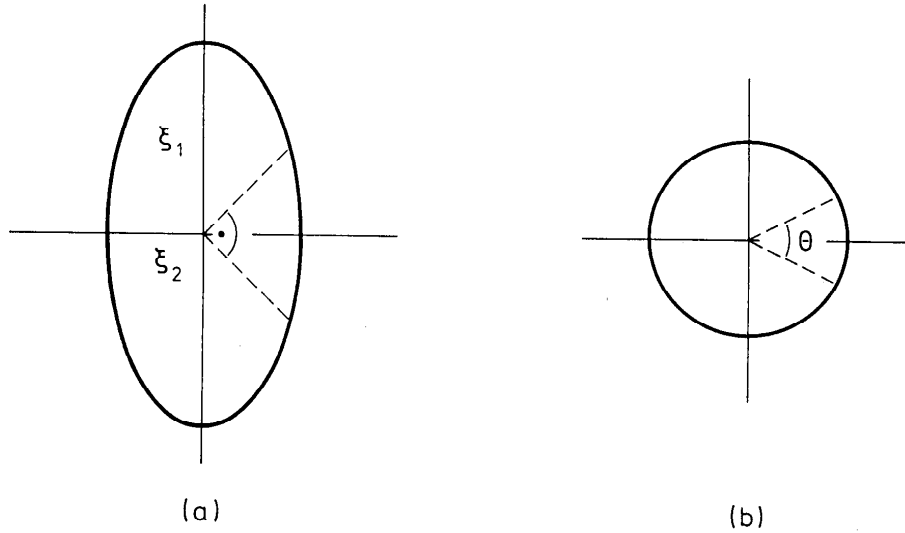


Figure B2. Rescaling of a system with different correlation lengths (a) into an isotropic one (b). The change of an angle is also indicated.

The results of the Hamiltonian limit may also be used to discuss isotropic systems. The problem becomes effectively isotropic if the correlation lengths in the two directions are rescaled as shown in Figure B2. For this, one introduces lattice constants a_i such that $a_1\xi_1 = a_2\xi_2$ [26, 31]. For the square lattice near criticality one has $\xi_2/\xi_1 = \cosh 2K_2/\cosh 2K_1 \cong 2K_1^* \ll 1$. Thus $a_2 = 1$ gives $a_1 = 2K_1^*$. The operator \mathcal{H} for row transfer then corresponds to a unit step in the isotropic system. For the wedge shown in the figure, the original opening angle of 90° is reduced to $\theta = 4K_1^*$. Therefore the operator \mathcal{H} for corner transfer corresponds to a step of twice the unit angle in the isotropic case. There is no change in the angle if the wedge is bounded by the principal axes.

Appendix C. Perturbation theory for extended defects

A perturbation approach to the extended defect critical behaviour has been proposed by Bariev [141]. It provides a criterion for marginal behaviour and, when the system is marginal, allows a determination of local first-order corrections to the scaling dimensions of either the order parameter $\sigma(\mathbf{r})$ or the energy density $\varepsilon(\mathbf{r})$. These corrections are obtained through a calculation of the two-point correlation functions to logarithmic accuracy, making use of the operator product expansion (OPE) [183, 184]. This is an extension to inhomogeneous systems of techniques introduced by Kadanoff and Wegner [185] in statistical physics and Polyakov [186] in quantum field theory. In the following the method is presented for a temperature-like extended perturbation and the correction to the order-parameter correlation function is determined.

C.1. General

One considers, in the continuum limit, the following perturbed d -dimensional system

$$-\beta\mathcal{H} = -\beta\mathcal{H}_0 + g \int \mathcal{Z}(\mathbf{r})\varepsilon(\mathbf{r})d\mathbf{r} \quad (C1)$$

where \mathcal{H}_0 is the unperturbed Hamiltonian and g the perturbation amplitude. The shape function $\mathcal{Z}(\mathbf{r})$, which gives the form of the inhomogeneity, is assumed to be homogeneous in r so that it may be generally written as

$$\mathcal{Z}(\mathbf{r}) = \frac{f(\mathbf{u})}{r^\omega} \quad (C2)$$

where \mathbf{u} is a unit vector along \mathbf{r} . The numerator contains the angular dependence of the perturbation which decays from the core of the defect with dimension d^* . For a point source $f(\mathbf{u}) = 1$ whereas for a line or a plane $f(\mathbf{u}) = |\cos \theta|^{-\omega}$ where θ is the angle measured from a polar axis which is orthogonal to the core subspace.

At the critical point of the unperturbed system the OPE is used, in multipoint correlation functions, to expand the product of two local operators at \mathbf{r}_1 and \mathbf{r}_2 on the complete set of operators associated with the fixed point of \mathcal{H}_0 . The distance r_{12} has to be smaller than the distances for other pairs appearing in the correlation function. Only the most singular term in the expansion is retained. The following reduction equations are needed:

$$\sigma(\mathbf{r}_1)\varepsilon(\mathbf{r}_2) \simeq a\sigma(\mathbf{r}_1)r_{12}^{-x} \quad \varepsilon(\mathbf{r}_1)\varepsilon(\mathbf{r}_2) \simeq b\varepsilon(\mathbf{r}_1)r_{12}^{-x} \quad (C3)$$

They are written for a translationally invariant system, x is the bulk scaling dimension of the energy density and averages are supposed to be subtracted. The powers in (C3) follow from scaling.

In a semi-infinite system translational invariance is lost in the direction perpendicular to the surface. When \mathbf{r}_1 belongs to the surface, the structure constants a and b in (C3) only acquire an angular dependence. When \mathbf{r}_2 goes to the surface, i.e. when $\theta \simeq \pi/2 - r_{12}^{-1}$, the surface scaling dimension d (Section 2.3), has to replace the bulk one in (C3). Then, as for surface scaling functions [18], one expects quite generally $a(\theta) \sim b(\theta) \sim (\cos \theta)^{d-x}$.

For the $2d$ Ising model with $x = 1$, one indeed obtains [187]

$$a(\theta) = \frac{2}{\pi} \cos \theta \quad b(\theta) = \frac{8}{\pi} \cos \theta \sin^2 \theta \quad (C4)$$

The bulk values are $a = 1/2\pi$ and $b = 0$. The last one vanishes due to the dual symmetry ($\varepsilon \rightarrow -\varepsilon$) of the bulk Ising model in two dimensions [156].

C.2. Relevance-irrelevance criterion

The order parameter correlation function has the following expansion in g

$$G(\mathbf{R}, g) = \sum_{n=0}^{\infty} \frac{g^n}{n!} \int_{\mathcal{E}'} \ll \sigma(0) \sigma(\mathbf{R}) \varepsilon(\mathbf{r}_1) \cdots \varepsilon(\mathbf{r}_n) \gg \prod_{i=1}^n \mathcal{Z}(\mathbf{r}_i) d\mathbf{r}_i \quad (C5)$$

where the double brackets denote the irreducible part of the multi-point correlation function. The integral extends over the subspace \mathcal{E}' with dimension d' where the perturbation is nonvanishing. \mathbf{R} is assumed to be orthogonal to the core subspace.

The OPE allows an evaluation of the first-order correction in (C5) giving

$$\delta G^{(1)} \sim g G(\mathbf{R}, 0) R^{d_{eff}-x} \quad (C6)$$

where x is the bulk scaling dimension of the energy density and, for a bulk perturbation, the effective dimension of the defect is defined as

$$d_{eff} = \max [d' - \omega, d^*] \quad (C7)$$

The second alternative, $d_{eff} = d^*$, is met when the angular integral in (C5) becomes divergent at $\theta = \pi/2$ due to the singularity of $\mathcal{Z}(\mathbf{r})$ at the core of the defect. This is cured by introducing a cut-off at $\theta = \pi/2 - r^{-1}$ which modifies the R -dependence in (C6) [141].

When $d_{eff} < x$, the leading correction to the long-distance behaviour is small and the perturbation is irrelevant. In the opposite case, the correction factor in (C6) grows

defect type	d^*	d'	d	d_{eff}
narrow line defect ($\omega = 0$)	1	1	2	1
surface extended line defect	1	2	2	$2 - \omega$
bulk extended line defect	1	2	2	$\max [2 - \omega, 1]$
radial defect	0	2	2	$2 - \omega$
surface field	0	1	2	$1 - \omega$

Table C1. Values of the effective dimension of the defects, d_{eff} , for the different systems studied in this review.

as a power of R , indicating a relevant perturbation and the expansion becomes useless. Finally, when $d_{eff} = x$, the perturbation is marginal and logarithmic corrections leading to g -dependent local exponents are obtained. As to the value of d_{eff} , Table C1 lists it for the systems studied in this review.

For slow decay (ω small), $d_{eff} = d' - \omega$, the perturbation is long-ranged and marginal behaviour sets in when $\omega = d' - x$. This is an extension to $d' < d$ of the condition obtained in (5.2) via scaling arguments. For large enough ω , $d_{eff} = d^*$, the perturbation is effectively short-ranged and one recovers the marginality criterion (6.5). Similar conclusions can be drawn for an order parameter perturbation as in Section 5.4.

With a free surface, the angular integral is modified through the angular dependence of the structure constants in (C4). As a result, d^* in (C7) has to be replaced by $d^* - d + x$ and marginal behaviour can no longer be induced by an effectively short-range defect since $d^* < d$.

C.3. Marginal behaviour

In the following, one assumes a bulk temperature-like perturbation and a defect with $d_{eff} = d' - \omega = x > d^*$. The n -th order term in (C5) can be rewritten so that the integration extends over $r_1 < r_2 \cdots < r_n$. The leading contribution to the multi-point function comes from pairs of points which are close to each other. Assuming that the shortest distance is between \mathbf{r}_1 and the origin and using the first reduction relation in (C3), the integral over \mathbf{r}_1 gives

$$a\sigma(0) \int_1^{r_2} dr_1 r_1^{d'-1-\omega-x} \int f(\mathbf{u}_1) d\mathbf{u}_1 \quad (C8)$$

where we wrote $d\mathbf{r}_1 = r_1^{d'-1} dr_1 d\mathbf{u}_1$ for the volume element. Since $d_{eff} > d^*$, the angular integral is regular and contributes a geometrical factor $S_{d'd^*}(\omega)$ leading to

$$\delta G^{(n)} = g^n a S_{d'd^*}(\omega) \int_{\mathcal{E}'(r_2 < r_3 \dots < r_n)} \ln r_2 \ll \sigma(0) \sigma(\mathbf{R}) \varepsilon(\mathbf{r}_2) \dots \varepsilon(\mathbf{r}_n) \gg \prod_{i=2}^n \mathcal{Z}(\mathbf{r}_i) d\mathbf{r}_i \quad (C9)$$

The same process can be iterated n times giving

$$\delta G^{(n)} = \frac{1}{n!} [ga S_{d'd^*}(\omega) \ln R]^n \ll \sigma(0) \sigma(\mathbf{R}) \gg \quad (C10)$$

It may be shown [141] that when other pairs like $\varepsilon(\mathbf{r}_1) \varepsilon(\mathbf{r}_2)$ are first contracted, the result is logarithmically smaller. Thus, to the leading logarithmic order, the perturbed correlation function is given by

$$G(\mathbf{R}, g) = G(\mathbf{R}, 0) R^{ga S_{d'd^*}(\omega)} \quad (C11)$$

From it, one deduces the first-order local change of the bulk order parameter scaling dimension x ,

$$x_l = x - ga S_{d'd^*}(\omega) + O(g^2) \quad (C12)$$

In the same way, for the local scaling dimension of the energy density, one obtains

$$x_l = x - gb S_{d'd^*}(\omega) + O(g^2) \quad (C13)$$

where x is the unperturbed bulk value [141].

These results are valid provided $|g| \ll 1$ and $|g| \ln^2 R \gg 1$ and can be used in the scaling region. When the two alternative conditions for marginal behaviour are simultaneously fulfilled, i.e. when $d' - \omega = d^* = x$, the perturbation results are only valid in a crossover regime with $|g| \ln R \ll 1$ and $|g| \ln^3 R \gg 1$ [187]. Then, due to the onset of local order at the bulk critical point when $g > 0$, the local dimensions are singular in g at $g = 0$ (see Section 7).

	point source	line source
bulk order parameter	$\frac{1}{8} - g$	—
surface order parameter	$\frac{1}{2} - \frac{4}{\pi}g$	$\frac{1}{2} - 2g$
surface energy density	$2 - \frac{16}{3\pi}g$	$2 - 4g$

Table C2. Local scaling dimensions for extended, temperature-like, marginal defects in the 2d Ising model, up to first order in the perturbation amplitude g .

In the semi-infinite geometry, with $d_{eff} = d' - \omega = x$, the calculation proceeds as in the bulk. The only change is introduced by the angular dependence of the structure constants [187]. Explicit results for marginal, bulk and surface extended perturbations in the two-dimensional Ising model are given in Table C2.

References

- [1] see for example 1976 *Phase Transitions and Critical Phenomena* vol 6 ed. C Domb and M S Green (London: Academic)
- [2] McCoy B M and Wu T T 1967 *Phys. Rev.* **162** 436
- [3] McCoy B M and Wu T T 1973 *The Two-Dimensional Ising Model* (Cambridge: Harvard University Press)
- [4] Binder K 1983 *Phase Transitions and Critical Phenomena* vol 8 ed. C Domb and J L Lebowitz (London: Academic) p 1
- [5] Diehl H W 1986 *Phase Transitions and Critical Phenomena* vol 10 ed. C Domb and J L Lebowitz (London: Academic) p 75
- [6] Baxter R J 1982 *Exactly Solved Models in Statistical Mechanics* (London: Academic)
- [7] Stinchcombe R B 1983 *Phase Transitions and Critical Phenomena* vol 7 ed. C Domb and J L Lebowitz (London: Academic) p 151
- [8] Wang J S, Selke W, Dotsenko V and Andreichenko V B 1990 *Physica* **164** 221
- [9] Abraham D B 1986 *Phase Transitions and Critical Phenomena* vol 10 ed. C Domb and J L Lebowitz (London: Academic) p 1
- [10] Jasnow D 1986 *Phase Transitions and Critical Phenomena* vol 10 ed. C Domb and J L Lebowitz (London: Academic) p 269
- [11] Forgács G, Lipowsky R and Nieuwenhuizen Th M 1991 *Phase Transitions and Critical Phenomena* vol 14 ed. C Domb and J L Lebowitz (London: Academic) p 135
- [12] Hoever P, Wolff W F and Zittartz J 1981 *Z. Phys. B* **41** 43
- [13] ——— 1981 *Z. Phys. B* **42** 259
- [14] ——— 1981 *Z. Phys. B* **44** 129
- [15] Bray A J and Moore M A 1977 *J. Phys. A: Math. Gen.* **10** 1927
- [16] Cardy J L 1987 *Phase Transitions and Critical Phenomena* vol 11 ed. C Domb and J L Lebowitz (London: Academic) p 55
- [17] Stella A L and Vanderzande C 1990 *Int. J. Mod. Phys. B* **4** 1437
- [18] Cardy J L 1984 *Nucl. Phys. B* **240** [FS12] 514
- [19] Burkhardt T W and Guim I 1991 *J. Phys. A: Math. Gen.* **24** 1557
- [20] Burkhardt T W, Eisenriegler E and Guim I 1989 *Nucl. Phys. B* **316** 559
- [21] Privman V 1985 *Phys. Rev. B* **32** 6089
- [22] Burkhardt T W and Eisenriegler E 1985 *J. Phys. A: Math. Gen.* **18** L83
- [23] Fisher M E and de Gennes P G 1978 *C. R. Acad. Sci., Paris B* **287** 207

- [24] Burkhardt T W and Cardy J L 1987 *J. Phys. A: Math. Gen.* **20** L233
- [25] Dietrich S and Diehl H W 1981 *Z. Phys. B* **43** 315
- [26] Cardy J L 1983 *J. Phys. A: Math. Gen.* **16** 3617
- [27] Duplantier B 1991 *Phys. Rev. Lett.* **66** 1555
- [28] Carslaw H S and Jaeger J C 1980 *Heat Conduction in Solids* (Oxford: Oxford University Press) chap. XIV
- [29] Smythe W R 1939 *Static and Dynamic Electricity* (New-York: McGraw-Hill) sect. 5.25
- [30] Jackson J D 1975 *Classical Electrodynamics* (New-York: Wiley) sect. 3.4
- [31] Barber M N, Peschel I and Pearce P A 1984 *J. Stat. Phys.* **37** 497
- [32] Peschel I 1985 *Phys. Lett.* **110A** 313
- [33] Kaiser C and Peschel I 1989 *J. Stat. Phys.* **54** 567
- [34] Davies B and Peschel I 1991 *J. Phys. A: Math. Gen.* **24** 1293
- [35] Peschel I and Truong T T 1987 *Z. Phys. B* **69** 385
- [36] de Gennes P-G 1979 *Scaling Concepts in Polymer Physics* (Ithaca and London: Cornell University Press) chap. X
- [37] Guttmann A J and Torrie G M 1984 *J. Phys. A: Math. Gen.* **17** 3539
- [38] Cardy J L and Redner S 1984 *J. Phys. A: Math. Gen.* **17** L933
- [39] Vanderzande C 1990 *J. Phys. A: Math. Gen.* **23** 563
- [40] Duplantier B and Saleur H 1986 *Phys. Rev. Lett.* **57** 3179
- [41] Considine D and Redner S 1989 *J. Phys. A: Math. Gen.* **22** 1621
- [42] Burkhardt T W and Guim I 1987 *Phys. Rev. B* **36** 2080
- [43] Burkhardt T W and Xue T 1991 *Phys. Rev. Lett.* **66** 895
- [44] ——— 1991 *Nucl. Phys. B* **354** 653
- [45] Cardy J L and Peschel I 1988 *Nucl. Phys. B* **300** [FS22] 377
- [46] Blöte H W J, Cardy J L and Nightingale M P 1986 *Phys. Rev. Lett.* **56** 742
- [47] Affleck I 1986 *Phys. Rev. Lett.* **56** 746
- [48] Cardy J L 1990 *Fields, Strings and Critical Phenomena* ed. E Brezin and J Zinn-Justin (Amsterdam: North-Holland) p 169
- [49] Kac M 1966 *Amer. Math. Monthly* **73** 1
- [50] McKean H P and Singer I M 1967 *J. Diff. Geom.* **1** 43
- [51] Baltes H P and Hilf E R 1976 *Spectra of Finite Systems* (Mannheim: Bibliogr. Institut) chap. VI
- [52] Peschel I 1988 *unpublished*
- [53] Gelfand M P and Fisher M E 1990 *Physica A* **166** 1
- [54] Kleban P and Vassileva I 1991 *J. Phys. A: Math. Gen.* **24** 3407

- [55] Privman V 1988 *Phys. Rev. B* **38** 9261
- [56] Peschel I, Turban L and Iglói F 1991 *J. Phys. A: Math. Gen.* **24** L1229
- [57] Blawid S 1993 *Diplomarbeit, Freie Universität Berlin*
- [58] Morse P M and Feshbach H 1953 *Methods of Theoretical Physics* (New-York: McGraw-Hill) chap. X
- [59] van Beijeren H 1977 *Phys. Rev. Lett.* **38** 933
- [60] Davies B and Peschel I 1992 *Ann. Physik* **2** 79
- [61] Binder K and Wang J S 1989 *J. Stat. Phys.* **55** 87
- [62] Hornreich R M, Luban M and Shtrikman S 1975 *Phys. Rev. Lett.* **35** 1678
- [63] Privman V and Švrakić N M 1989 *Directed Models of Polymers, Interfaces and Clusters* Lecture Notes in Physics vol 338 (Berlin: Springer)
- [64] Turban L 1992 *J. Phys. A: Math. Gen.* **25** L127
- [65] Iglói F 1992 *Phys. Rev. A* **45** 7024
- [66] Turban L and Berche B 1993 *J. Phys. I France* **3** 925
- [67] Burkhardt T W 1982 *Phys. Rev. Lett* **48** 216
- [68] Cordery R 1982 *Phys. Rev. Lett* **48** 215
- [69] Hilhorst H J and van Leeuwen J M J 1981 *Phys. Rev. Lett.* **47** 1188
- [70] Syozi I 1972 *Phase Transitions and Critical Phenomena* vol 1 ed. C. Domb and M.S. Green (London: Academic) p 269
- [71] Burkhardt T W and Guim I 1984 *Phys. Rev. B* **29** 508
- [72] Burkhardt T W, Guim I, Hilhorst H J and van Leeuwen J M J 1984 *Phys. Rev. B* **30** 1486
- [73] Blöte H W J and Hilhorst H J 1983 *Phys. Rev. Lett.* **51** 20
- [74] ——— 1985 *J. Phys. A: Math. Gen.* **18** 3039
- [75] Luther A and Peschel I 1975 *Phys. Rev. B* **12** 3908
- [76] Iglói F and Turban L 1993 *Phys. Rev. B* **47** 3404
- [77] Fisher M E 1974 *Renormalization Group in Critical Phenomena and Quantum Field Theory* Proceedings of a Conference ed. J D Gunton and M S Green (Philadelphia: Temple University Press) p 65
- [78] Abraham DB 1971 *Stud. Appl. Math.* **50** 71
- [79] Peschel I 1984 *Phys. Rev. B* **30** 6783
- [80] Lieb E H, Schultz T D and Mattis D C 1961 *Ann. Phys. (N. Y.)* **16** 406
- [81] Abramowitz M and Stegun I A 1965 *Handbook of Mathematical Functions* (New York: Dover)
- [82] Turban L and Berche B 1993 *J. Phys. A: Math. Gen.* **26** 3131
- [83] Burkhardt T W and Iglói F 1990 *J. Phys. A: Math. Gen.* **23** L633

- [84] Burkhardt T W and Guim I 1985 *J. Phys. A: Math. Gen.* **18** L25
- [85] Iglói F 1990 *Phys. Rev. Lett.* **64** 3035
- [86] Berche B and Turban L 1990 *J. Phys. A: Math. Gen.* **23** 3029
- [87] Choi J-Y 1993 *J. Phys. A: Math. Gen.* **26** L327
- [88] Burkhardt T W and Guim I 1982 *J. Phys. A: Math. Gen.* **15** L305
- [89] Iglói F 1992 *Europhys. Lett.* **19** 305
- [90] Bariev R Z and Peschel I 1991 *Phys. Lett.* **153A** 166
- [91] Luck J M 1993 *J. Stat. Phys.* **72** 417
- [92] Iglói F 1993 *J. Phys. A: Math. Gen.* **26** L703
- [93] Harris A B 1974 *J. Phys. C: Solid State Phys.* **7** 1671
- [94] Turban L and Berche B 1993 *Z. Phys. B* **92** 307
- [95] Hucht A 1992 *Physica* **A183** 223
- [96] Wildpaner V, Rauch H and Binder K 1973 *J. Phys. Chem. Solids* **34** 925
- [97] Binder K, Stauffer D and Wildpaner V 1975 *Acta Met.* **23** 119
- [98] Burkhardt T W and Eisenriegler E 1981 *Phys. Rev. B* **24** 1236
- [99] Eisenriegler E and Burkhardt T W 1982 *Phys. Rev. B* **25** 3283
- [100] Diehl H W, Dietrich S and Eisenriegler E 1983 *Phys. Rev. B* **27** 2937
- [101] Abe R 1981 *Prog. Theor. Phys.* **65** 1237
- [102] ——— 1981 *Prog. Theor. Phys.* **65** 1835
- [103] Yamamoto K and Abe R 1981 *Prog. Theor. Phys.* **66** 1947
- [104] Abe R and Yamamoto K 1982 *Prog. Theor. Phys.* **67** 139
- [105] Abe R, Yamamoto K and Ideura K 1983 *Prog. Theor. Phys.* **69** 464
- [106] Ideura K and Abe R 1984 *Prog. Theor. Phys.* **71** 27
- [107] Ideura K 1984 *Prog. Theor. Phys.* **71** 474
- [108] Bariev R Z 1979 *Zh. Eksp. Teor. Fiz.* **77** 1217
[*Sov. Phys. JETP* **50** 613 (1979)]
- [109] McCoy B M and Perk J H H 1980 *Phys. Rev. Lett.* **44** 840
- [110] Fisher M E and Ferdinand A E 1967 *Phys. Rev. Lett.* **19** 169
- [111] Ko L-F, Au-Yang H and Perk J H H 1985 *Phys. Rev. Lett.* **54** 1091
- [112] Kadanoff L P 1981 *Phys. Rev. B* **24** 5382
- [113] Brown A C 1982 *Phys. Rev. B* **25** 331
- [114] Burkhardt T W and Choi J-Y 1992 *Nucl. Phys. B* **376** 447
- [115] Abraham D B, Ko L-F and Švrakić N M 1988 *Phys. Rev. Lett.* **61** 2393
- [116] Uzelac K, Jullien R and Pfeuty P 1981 *J. Phys. A: Math. Gen.* **14** L17
- [117] Turban L 1982 *J. Phys. A: Math. Gen.* **15** 1733
- [118] Nozières P and de Dominicis C T 1969 *Phys. Rev.* **178** 1097

- [119] Peschel I and Schotte K D 1984 *Z. Phys. B* **54** 305
- [120] Cabrera G G and Jullien R 1986 *Phys. Rev. Lett.* **57** 393
- [121] Zinn-Justin J 1986 *Phys. Rev. Lett.* **57** 3296
- [122] Cabrera G G and Jullien R 1987 *Phys. Rev. B* **36** 7062
- [123] Barber M N and Cates M E 1987 *Phys. Rev. B* **36** 2024
- [124] Iglói F 1989 *Phys. Rev. B* **40** 5187
- [125] Nightingale M P and Blöte H W J 1982 *J. Phys. A: Math. Gen.* **15** L33
- [126] Kaufman M and Griffiths R B 1982 *Phys. Rev. B* **26** 5282
- [127] Turban L 1985 *J. Phys. A: Math. Gen.* **18** L325
- [128] Guimarães L G and Drugowich de Felicio J R 1986 *J. Phys. A: Math. Gen.* **19** L341
- [129] Henkel M and Patkós A 1987 *J. Phys. A: Math. Gen.* **20** 2199
- [130] Henkel M, Patkós A and Schlottmann M 1989 *Nucl. Phys. B* **314** 609
- [131] Henkel M and Patkós A 1988 *J. Phys. A: Math. Gen.* **21** L231
- [132] Irving A C, Ódor G and Patkós A 1989 *J. Phys. A: Math. Gen.* **22** 4665
- [133] Henkel M and Patkós A 1987 *Nucl. Phys. B* **285** 29
- [134] Baake M, Chaselon P and Schlottmann M 1989 *Nucl. Phys. B* **314** 625
- [135] Henkel M 1990 *Finite-Size Scaling and Numerical Simulations of Statistical Systems* ed. V Privman (Singapore: World Scientific) chap. VIII
- [136] Schlottmann M 1988 *Diplomarbeit Bonn-IR-88-41*
- [137] Grimm U 1990 *Nucl. Phys. B* **340** 633
- [138] Wittlich T 1990 *J. Phys. A: Math. Gen.* **23** 3825
- [139] Grimm U 1988 *Diplomarbeit Bonn-IR-88-30*
- [140] Hinrichsen H 1990 *Nucl. Phys. B* **336** 377
- [141] Bariev R Z 1988 *Zh. Eksp. Teor. Fiz.* **94** 374
[*Sov. Phys. JETP* **67** 2170 (1988)]
- [142] ——— 1989 *J. Phys. A: Math. Gen.* **22** L397
- [143] Bariev R Z and Malov O A 1989 *Phys. Lett.* **136A** 291
- [144] Bariev R Z and Ilaldinov I Z 1989 *J. Phys. A: Math. Gen.* **22** L879
- [145] Iglói F, Berche B and Turban L 1990 *Phys. Rev. Lett.* **65** 1773
- [146] Burkhardt T W 1984 *Phase Transitions in Disordered Systems* Lecture Notes in Physics vol 206 ed. A Pekalski and J Sznajd (Berlin: Springer)
- [147] Peschel I and Wunderling R 1992 *Ann. Physik* **1** 125
- [148] Peschel I and Truong T T 1991 *Ann. Physik* **48** 185
- [149] Bariev R Z and Peschel I 1991 *J. Phys. A: Math. Gen.* **24** L87
- [150] Turban L 1991 *Phys. Rev. B* **44** 7051
- [151] Privman V and Fisher M E 1984 *Phys. Rev. B* **30** 322

- [152] Hamer C J and Barber M N 1981 *J. Phys. A: Math. Gen.* **14** 241
- [153] Henkel M 1987 *J. Phys. A: Math. Gen.* **20** 995
- [154] Burkhardt T W and Guim I 1987 *Phys. Rev. B* **35** 1799
- [155] Reinicke P 1987 *J. Phys. A: Math. Gen.* **20** 4501
- [156] Kramers H A and Wannier G 1941 *Phys. Rev.* **60** 252
- [157] Saleur H 1988 *J. Phys. A: Math. Gen.* **22** L41
- [158] Saleur H and Bauer M 1989 *Nucl. Phys. B* **320** 591
- [159] Fisher M E 1971 *Critical Phenomena* ed. M S Green (London: Academic) p 1
- [160] Polyakov A M 1970 *Zh. Eksp. Teor. Fiz. Pis. Red.* **12** 538
[*Sov. Phys. JETP Lett.* **12** 381 (1970)]
- [161] Belavin A A, Polyakov A M and Zamolodchikov A B 1984 *J Stat Phys* **34** 763
- [162] for a pedagogical introduction to the subject, see Christe P and Henkel M 1993
Introduction to Conformal Invariance and its Applications to Critical Phenomena
Lecture Notes in Physics vol m16 (Berlin: Springer)
- [163] Friedan D, Qiu Z and Shenker S 1984 *Phys. Rev. Lett.* **52** 1575
- [164] Cardy J L 1984 *J. Phys. A: Math. Gen.* **17** L385
- [165] Montroll E W 1941 *J. Chem. Phys.* **9** 706
- [166] Lassetre E N and Howe J P 1941 *J. Chem. Phys.* **9** 747
- [167] Schultz T D, Mattis D C and Lieb E H 1964 *Rev. Mod. Phys.* **36** 856
- [168] Kaufman B 1949 *Phys. Rev.* **76** 1232
- [169] Fradkin E and Susskind L 1978 *Phys. Rev. D* **17** 2637
- [170] Kogut J B 1979 *Rev. Mod. Phys.* **51** 659
- [171] Jordan P and Wigner E 1928 *Z. Phys.* **47** 631
- [172] Pfeuty P 1970 *Ann. Phys. (N. Y.)* **57** 79
- [173] Katsura S 1962 *Phys. Rev.* **127** 1508
- [174] Onsager L 1944 *Phys. Rev.* **65** 117
- [175] Baxter R J 1977 *J. Stat. Phys.* **17** 1
- [176] Baxter R J 1981 *Physica* **106A** 18
- [177] Baxter R J 1985 *Integrable Systems in Statistical Mechanics VII* ed. G M d'Ariano,
A Monerosi and M G Rasetti (Singapore: World Scientific)
- [178] Davies B 1988 *Physica* **154A** 1
- [179] Truong T T and Peschel I 1989 *Z. Phys. B* **75** 119
- [180] Peschel I 1988 *J. Phys. A: Math. Gen.* **21** L185
- [181] Davies B and Pearce P A 1990 *J. Phys. A: Math. Gen.* **23** 1295
- [182] Onsager L 1949 *Nuovo Cim. (Suppl.)* **6** 201
- [183] Polyakov A M 1969 *Zh. Eksp. Teor. Fiz.* **57** 271

- [Sov. Phys. *JETP* **30** 151 (1969)]
- [184] Kadanoff L P and Ceva H 1971 *Phys. Rev. B* **3** 3918
- [185] Kadanoff L P and Wegner F J 1971 *Phys. Rev. B* **4** 3989
- [186] Polyakov A M 1972 *Zh. Eksp. Teor. Fiz.* **63** 24
[Sov. Phys. *JETP* **36** 12 (1972)]
- [187] Bariev R Z and Turban L 1992 *Phys. Rev. B* **45** 10761